Gas Generation Testing of Crystalline Silicotitanate Ion Exchange Media

July 2019

HA Colburn
AM Rovira
SR Adami
DM Camaioni
SA Bryan
PP Schonewill

U.S. DEPARTMENT OF **ENERGY**

DISCLAIMER

This report was prepared as an account of work sponsored by an agency of the United States Government. Neither the United States Government nor any agency thereof, nor Battelle Memorial Institute, nor any of their employees, **makes any warranty, express or implied, or assumes any legal liability or responsibility for the accuracy, completeness, or usefulness of any information, apparatus, product, or process disclosed, or represents that its use would not infringe privately owned rights**. Reference herein to any specific commercial product, process, or service by trade name, trademark, manufacturer, or otherwise does not necessarily constitute or imply its endorsement, recommendation, or favoring by the United States Government or any agency thereof, or Battelle Memorial Institute. The views and opinions of authors expressed herein do not necessarily state or reflect those of the United States Government or any agency thereof.

PACIFIC NORTHWEST NATIONAL LABORATORY
operated by
BATTELLE
for the
UNITED STATES DEPARTMENT OF ENERGY
under Contract DE-AC05-76RL01830

Printed in the United States of America

Available to DOE and DOE contractors from
the Office of Scientific and Technical
Information,
P.O. Box 62, Oak Ridge, TN 37831-0062
www.osti.gov
ph: (865) 576-8401
fox: (865) 576-5728
email: reports@osti.gov

Available to the public from the National Technical Information Service
5301 Shawnee Rd., Alexandria, VA 22312
ph: (800) 553-NTIS (6847)
or (703) 605-6000
email: info@ntis.gov
Online ordering: http://www.ntis.gov

Gas Generation Testing of Crystalline Silicotitanate Ion Exchange Media

July 2019

HA Colburn
AM Rovira
SR Adami
DM Camaioni
SA Bryan
PP Schonewill

Pacific Northwest National Laboratory
Richland, Washington 99354

Summary

The Direct Feed Low-Activity Waste (DFLAW) process has been proposed to support early production of immobilized low-activity waste (LAW) at the Hanford site. As planned, Hanford tank waste would be sent to the Tank Side Cesium Removal (TSCR) system for solids removal (by filtration) and cesium removal (by ion exchange) during the initial phase of the DFLAW process. The resultant treated waste would be delivered to the LAW Vitrification Facility at the Hanford Tank Waste Treatment and Immobilization Plant (WTP) for immobilization. The ongoing technology maturation of TSCR system components is being conducted by Washington River Protection Solutions, LLC (WRPS).

The ion exchange process in the TSCR system will use columns of crystalline silicotitanate (CST) to remove cesium from the LAW. This report describes gas generation testing of the crystalline silicotitanate ion exchange media that was conducted to strengthen the technical basis of the media for use in the TSCR system. Specifically, the described study will inform the safety basis of both the operation of the TSCR system and the interim storage condition of the TSCR ion exchange columns after loading. Previous data on gas generation of CST are limited to a handful of studies using CST or similar media under unrepresentative conditions and durations. The safety basis underlying operation and storage of the CST columns needs to consider the rate and extent of radiolytic flammable gas generation. No existing studies provide a comprehensive set of gas generation data for column operating and storage conditions representative of those expected for TSCR. To address the data gap, this study was conducted under the following conditions (each in duplicate):

- CST in water at 25°C tested to 300 Mrad total dose

- wet CST (soaked in water, then free-drained) at 25°C tested to both 300 Mrad and 900 Mrad total dose

- dry CST (air-dried, free-flowing material equilibrated to laboratory conditions) at 25°C tested to both 300 Mrad and 900 Mrad total dose

- CST in 5.6M Na simulant at 25°C tested to 300 Mrad total dose

- CST in 5.6M Na simulant with 1% (w/w) total organic carbon as Na_3-HEDTA at 25°C and 70°C tested to 300 Mrad total dose.

For each of the listed conditions, the generation of the following gas species was measured: hydrogen, oxygen, nitrous oxide, and methane. The test data was used to determine the amount of gas generated (total and on a per-component basis), gas generation rates normalized to the CST bed volume tested, and G-values[1] for each gas species. The reported results illustrate that the CST-in-water condition bounds the gas generation rate (at 25°C) of all other conditions, but there is some variability in the hydrogen G-value, depending on the lot of CST tested and the amount of residual moisture present at the start of the test.

---

[1] The G-value is a measure of the amount of gas generated per dose absorbed. In this study, PNNL speciated the gases generated, so G-values for gases of interest are reported as molecules per 100 eV absorbed dose.

Acknowledgments

Acronyms and Abbreviations

CST	crystalline silicotitanate
DFLAW	Direct Feed Low-Activity Waste
DI	deionized
DOE-ORP	U.S. Department of Energy Office of River Protection
FIO	for information only
G-value	a constant in the radiolysis rate equation for gas generation, it represents a measure of the amount of gas generated per radiation dose absorbed
HEDTA	N-(2-hydroxyethyl)ethylenediaminetriacetic acid
ICP-OES	inductively coupled plasma optical emission spectroscopy
LAW	low-activity waste
LAWPS	Low-Activity Waste Pretreatment System
MCNP	Monte Carlo N-particle transport code
NIST	National Institute of Standards and Technology
PNNL	Pacific Northwest National Laboratory
QA	quality assurance
R&D	research and development
RPL	Radiochemical Processing Laboratory
sRF	spherical resorcinol-formaldehyde
SRNL	Savannah River National Laboratory
TCCR	Tank Closure Cesium Removal
TGA	thermogravimetric analysis
TOC	total organic carbon
TSCR	Tank Side Cesium Removal
WRPS	Washington River Protection Solutions, LLC
WTP	Hanford Tank Waste Treatment and Immobilization Plant
WWFTP	WRPS Waste Form Testing Program

Contents

Figures

Tables

1.0 Introduction

The primary mission of the U.S. Department of Energy Office of River Protection (DOE-ORP) is to retrieve and process approximately 56 million gallons of radioactive waste from 177 underground tanks located on the Hanford Site. The Hanford waste tanks are currently operated and managed by Washington River Protection Solutions, LLC (WRPS). As part of tank farm operations, WRPS supports DOE-ORP's waste retrieval mission. An important element of the DOE-ORP mission is the construction and operation of the Hanford Tank Waste Treatment and Immobilization Plant (WTP). The WTP is tasked with separating the waste into low-activity waste (LAW) and high-level waste fractions and immobilizing these fractions by vitrification. The primary contractor supporting the construction of the WTP is Bechtel National, Inc.

To support early production of immobilized LAW, the Direct Feed Low-Activity Waste (DFLAW) process has been proposed (Tilanus et al. 2017). As planned, in the initial phase of the DFLAW process, supernatant would be sent to the Tank Side Cesium Removal (TSCR) system for solids removal by filtration and cesium removal by ion exchange (for a flowsheet overview, see Anderson 2018). The resultant treated waste would be delivered to the WTP LAW Vitrification Facility for immobilization. The design of the TSCR system is being conducted by AVANTech, Inc., at the direction of WRPS (see the specification outlined in Ard 2019). The TSCR system shares many similarities with the Tank Closure Cesium Removal (TCCR) system recently demonstrated at the Savannah River site; refer to King et al. (2018a) for some supporting data, or Chew et al. 2019 for a discussion of how TCCR fits into the Savannah River site plan for liquid waste treatment.

In both the TSCR and TCCR systems, the ion exchange function is performed using crystalline silicotitanate (CST). CST is highly selective for cesium and has been tested extensively at multiple sites across the DOE complex, most notably in a demonstration effort to treat Melton Valley storage tank waste at Oak Ridge National Laboratory (Walker et al. 1998). It has also recently been deployed in one of the treatment systems used for cleanup after the nuclear accident in Fukushima, Japan (Braun and Barker 2012). In anticipation of production-scale use of CST on the Hanford Site, Pacific Northwest National Laboratory (PNNL) compiled a comprehensive summary of data and operational information that has been collected about CST since the early 1990s, as well as uncertainties with regard to its expected performance in its planned Hanford application (Pease et al. 2019). The summary of the state of the art by Pease et al. identified a few areas in which collecting data could reduce CST performance uncertainty or support safe operation of the TSCR system (or a similar facility using CST).

One important area where more information was warranted was data describing how the presence of CST impacts the generation of flammable gases. To that end, WRPS identified gas generation testing as a component of the technical maturation of the TSCR system (and, more generally, the use of CST). Gas generation during TSCR operations can conceivably come from three main sources: thermal degradation of organic species, radiolytic degradation (both of water and organic species), and corrosion processes. Some of the constituents of tank wastes inhibit corrosion and radiolytic generation of hydrogen (e.g., NO_2^- and NO_3^-). However, the condition of greatest interest is the gas generation behavior when the CST bed still contains water but is not fully saturated. These conditions mimic expected TSCR column operations when the ion exchange process is deemed complete and the columns are being prepared for interim storage. At that point, the waste being processed is displaced by 0.1M NaOH, rinsed with water, and then bulk dewatered with compressed air. The CST bed will contain residual amounts of moisture depending on how long compressed air is used to dry the bed.

The generation of flammable gas with CST has been investigated previously; data have primarily been reported by researchers at Savannah River National Laboratory (SRNL). The work of McCabe (1997),

Bibler et al. (1998), Walker et al. (1999), Hamm et al. (2002), Walker (2003), and McCabe (2004) are all of interest. Note that none of these studies used Hanford waste (or designed a simulant based on relevant Hanford waste chemistry), fully speciated the gas generated, irradiated past a period of approximately one week, used recently manufactured lots of CST media, or measured gas generation rates in CST beds that were not fully saturated with water. For all these reasons, it was determined that additional data were needed. The data that were collected, particularly by Bibler et al., are a useful reference as they report results at similar conditions such as a range of water/CST slurries (13 to 83 wt% water), a sodium hydroxide/CST slurry, and a salt solution/CST slurry containing nitrate and nitrite; they were used to compare against the data collected from the fully saturated CST bed of the current study.

To bound the range of possible moisture content, PNNL tested CST at conditions ranging from CST that was fully saturated with water to CST that was equilibrated with ambient air for a period of several days (nominally dry). Additionally, the gas generation behavior was tested in conditions representing normal operations during waste processing. For these tests, the CST was saturated with a chemically representative waste simulant with and without a significant organic component. Testing was conducted in a manner similar to the approach described by Colburn et al. (2018).

The ensuing sections of this report provide a description of the quality assurance applicable to PNNL's work (Section 2.0) and a brief description of a preliminary modeling exercise conducted to estimate the expected dose rate (Section 3.0). The bulk of the report describes the experimental conditions, including the collection and analysis of data (Section 4.0), the resulting gas generation rates (Section 5.0), and characterization of CST moisture content (Section 6.0). In Section 7.0, the testing is summarized with some concluding remarks. Appendices A through C, respectively, contain the detailed gas composition analysis results, TSCR column dose modeling information, and source calibration information.

2.0 Quality Assurance

This work was conducted with funding from WRPS under Contract 36437-251, "LAWPS Technology Testing and Support," for the Low-Activity Waste Pretreatment System (LAWPS) Technology Testing and Support Project. The work was conducted as part of PNNL project number 72195.

All research and development (R&D) work at PNNL is performed in accordance with PNNL's Laboratory-Level Quality Management Program, which is based on a graded application of NQA-1-2000, *Quality Assurance Requirements for Nuclear Facility Applications*, to R&D activities. To ensure that all client quality assurance (QA) expectations were addressed, the QA controls of the WRPS Waste Form Testing Program (WWFTP) QA program were also implemented for this work. The WWFTP QA program implements the requirements of NQA-1-2008, *Quality Assurance Requirements for Nuclear Facility Applications*, and NQA-1a-2009, *Addenda to ASME NQA-1-2008*, and consists of the WWFTP Quality Assurance Plan (QA-WWFTP-001) and associated QA-NSLW-numbered procedures that provide detailed instructions for implementing NQA-1 requirements for R&D work.

Specific details of this project's approach to assuring quality are contained in the LAWPS Testing Program Quality Assurance Plan (72195-QA-001, Rev. 2) and associated implementing procedures. The QA plan describes how the procedures of the WWFTP QA program were used when conducting the work. The work described in this report was assigned the technology level "Applied Research," and was planned, performed, documented, and reported in accordance with procedure QA-NSLW-1102, *Scientific Investigation for Applied Research*. All staff members contributing to the work received proper technical and QA training prior to performing quality-affecting work.

3.0 TSCR Column Dose Modeling

NOTE: The modeling results presented in this section are for information only (FIO). The work described in this section uses the Monte Carlo N-Particle (MCNP®)[1] transport code widely used across the DOE complex to model neutron, photon, electron, and coupled transport. However, the software was not verified or validated for use under the QA program described in Section 2.0 and thus, despite the modeling being conducted in a manner consistent with PNNL procedures and best practices, must be considered FIO.

An important consideration with respect to selecting conditions for gas generation testing is to perform experiments at irradiation rates that are consistent with the expected dose rate in the TSCR operating environment. To support the testing described in the rest of this report, a model assessment using MCNP was devised using the most current information about the proposed TSCR columns at the start of gas generation testing (approximately June 2018).[2]

Based on a range of assumed liquid densities in the column between 1.00 and 1.27 g/mL, a series of estimates of the total dose that would occur over a 60-day period, assuming an instantaneous loading of 150,000 Ci, was generated. The nominal irradiation rate was then estimated by assuming a uniform emission of radiation over the 60-day period. The irradiation rates obtained by this approach varied from 313 to 337 krad/hr. The model values are on the same order as the irradiation rates used in the gas generation experiments, but are approximately a factor of two (~39 to 47%) lower than the experimental values.[3] The experimental irradiation rates, therefore, are bounding with respect to the predictions of a simple model estimate generated based on conservative assumptions. Additional details and descriptions of the dose modeling approach, inputs, and results are available in Appendix B.

---

[1] Both Monte Carlo N-Particle and MCNP® are registered trademarks owned by Triad National Security, LLC. For more information, see https://mcnp.lanl.gov/.

[2] In an e-mail from Matthew R. Landon (WRPS) to Philip P. Schonewill (PNNL) on September 19, 2018, titled *"FW: 30% design review,"* WRPS provided PNNL with a draft drawing "H-14-111250 Rev. A Sheet 1.pdf." As of June 2018, that drawing was still understood to represent the planned TSCR column geometry.

[3] Based on the extrema of model values (313 to 337 krad/hr) and average experimental values from the testing (556 to 588 krad/hr), the difference between the values ranges from (588 – 313)/588 = ~47% to (556 – 337)/556 = ~39%.

4.0   Experimental

PNNL has conducted various gas generation measurements using actual Hanford tank waste for more than 20 years. Recently, PNNL determined the gas generation rates of spherical resorcinol-formaldehyde (sRF) resin in a variety of potential process liquids and temperatures (Colburn et al. 2018). The tests used equipment that was designed and built based on previous gas generation testing performed during the period of 1996–1999, in which gas generation rates were measured for six Hanford tank waste types with and without external radiation exposure (Bryan and Pederson 1994, 1995; Bryan et al. 1996; King et al. 1997; King and Bryan 1998 (not publically available)[1], 1999). This section summarizes the equipment and methods used to collect data for the current work with CST media; many of the elements used in the current testing were similar (or identical) to those used in the cited PNNL work.

4.1   Experimental Conditions and Equipment

The gas generation testing equipment used in the current testing was the same equipment used in previous ion exchange media gas generation testing (Colburn et al. 2018). The equipment comprises two functionally identical systems: one for the vessels exposed to a Co-60 radiation source (the "Rad system") and one for the thermal-only testing (the "Thermal system"). As with the previous work, sample irradiation experiments were performed at the High Exposure Facility within the 318 Building at PNNL. Due to the long duration of the irradiation exposures (21 to 70 days), the gamma bunker in the High Exposure Facility was used to house the gas generation experiment payload (a carousel of eight sample vessels) with a ~2,500 Ci Co-60 source centered on the gas generation test vessels. The bunker provides 8 in. of solid poured lead for shielding all the way around the sample carousel. The primary changes to the system from the one delineated by Colburn et al. (2018) included the use of a higher activity Co-60 source and the incorporation of a chiller (Figure 4.1) and cooling loop (Figure 4.2) on the sample carousel to better maintain the temperature inside of the bunker.

---

[1]   King CM and SA Bryan. 1998. *Thermal and Radiolytic Gas Generation from Tank 241-A-101 Waste: Status Report*. TWS98.78, Pacific Northwest National Laboratory, Richland, Washington.

Figure 4.1. Rad system bunker with the updated chiller installed
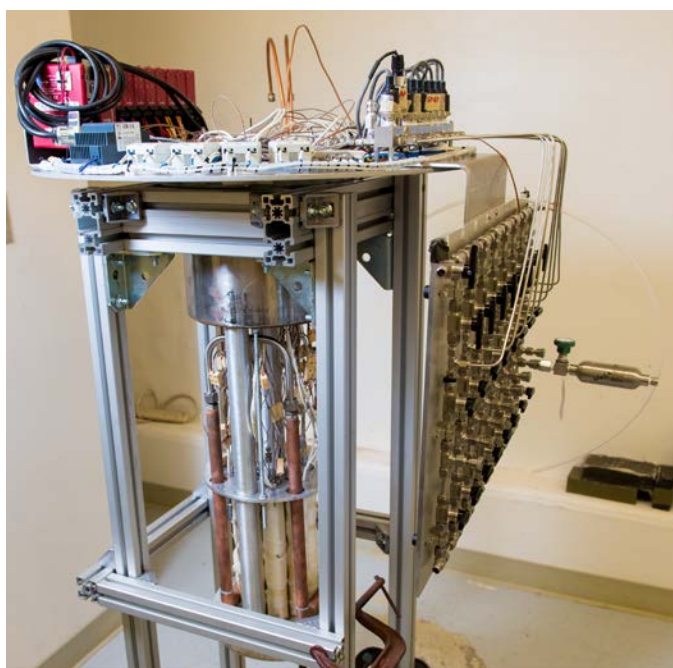
Figure 4.2. Bunker payload with the cooling loop in place

4.2 Simulant Preparation and CST Handling

The gas generation testing used waste simulants for some of the test conditions. The preparation of these simulants is described in Section 4.2.1. Prior to loading the vessels for each test, the CST was pretreated

as discussed Section 4.2.2. The pretreatment varied slightly depending on the test condition; in some cases, samples were collected during the pretreatment activity to measure moisture content. Section 4.2.3 briefly describes the loading of test vessels with CST and process fluids.

4.2.1 Simulant Preparation

Gas generation testing employed a 5.6M sodium chemical simulant that has been historically used to evaluate TSCR and related low-activity waste pre-treatment unit operations. This simulant was developed as discussed in Russell et al. (2017); note that in the current testing, the 5.6M Na simulant was prepared without oxalate. Although the simulant recipe calls for oxalate, it was excluded in order to isolate the impact of the inorganic salt species. Simulant preparation was conducted using American Chemical Society reagent grade materials. For simulants containing added NaOH, the NaOH was added in the form of a commercially supplied 50% (w/w) solution. All other components were obtained and added directly as salts. The final volume was obtained through the addition of deionized (DI) water.

The nominal and as-prepared compositions are listed in Table 4.1. The simulant was submitted to PNNL's 331 Analytical Services Laboratory for anion and cation analysis by ion chromatography and inductively coupled plasma optical emission spectroscopy (ICP-OES), respectively. The analytical results for the prepared simulant are also presented in Table 4.1. Further gas generation testing was conducted using the same 5.6M Na simulant with additional 1% (w/w) organic carbon as Na_3-HEDTA. The sodium salt of HEDTA was chosen as the organic carbon additive in concurrence with WRPS because it is known to generate gas under radiolysis in Hanford tank waste (Bryan and Pederson 1994). It also produces N_2O, which is important for assessing flammability in oxygen-deficient environments (Mahoney 2015), and permits comparison with prior experimental work performed with the same simulant (Colburn et al. 2018). The nominal and as-prepared concentrations of the HEDTA-containing simulant are listed in Table 4.2. Due to the similarity of the simulants (5.6M Na and 5.6M Na with 1% organic carbon), the organic carbon-bearing simulant was not verified by analytical measurements.

Table 4.1. Nominal, as prepared, and analyzed composition of the 5.6M Na LAWPS simulant without oxalate

Dissolved Species	Nominal Concentration (M)	As Prepared (M)	Analyzed Concentration (M)
Al	1.66×10^{-1}	1.67×10^{-1}	1.85×10^{-1}
Cs	1.04×10^{-4}	9.90×10^{-5}	Not measured
Nitrate	1.78×10^{0}	1.78×10^{0}	1.79×10^{0}
Nitrite	1.02×10^{0}	1.02×10^{0}	1.07×10^{0}
Phosphate	4.32×10^{-2}	4.33×10^{-2}	4.49×10^{-2}
Sulfate	6.61×10^{-2}	6.62×10^{-2}	6.84×10^{-2}
Inorganic C	4.67×10^{-1}	4.68×10^{-1}	Not measured
Chloride	1.22×10^{-1}	1.23×10^{-1}	1.25×10^{-1}
Free Hydroxide	1.41×10^{0}	1.40×10^{0}	Not measured
Potassium	1.22×10^{-1}	1.23×10^{-1}	1.21×10^{-1}
Sodium	5.57×10^{0}	5.57×10^{0}	5.83×10^{0}

Table 4.2. Nominal and as prepared composition of the 5.6M Na LAWPS simulant with 1% (w/w) total organic carbon (TOC) as Na$_3$-HEDTA

Dissolved Species	Recipe Concentration (M)	As Prepared (M)
Al	1.66×10^{-1}	1.67×10^{-1}
Cs	1.04×10^{-4}	9.90×10^{-5}
Nitrate	1.78×10^{0}	1.78×10^{0}
Nitrite	1.02×10^{0}	1.02×10^{0}
Phosphate	4.32×10^{-2}	4.33×10^{-2}
Sulfate	6.61×10^{-2}	6.62×10^{-2}
Inorganic C	4.67×10^{-1}	4.68×10^{-1}
Organic C	1.04×10^{0}	1.04×10^{0}
Chloride	1.22×10^{-1}	1.23×10^{-1}
Free hydroxide	1.41×10^{0}	1.40×10^{0}
Potassium	1.22×10^{-1}	1.23×10^{-1}
Sodium	5.88×10^{0}	5.88×10^{0}

4.2.2   CST Handling and Preparation

The CST for gas generation testing was used as-received and unsieved. CST was provided for testing by WRPS, who obtained the material from the manufacturer, Honeywell UOP (Des Plaines, Illinois). The first test used CST IONSIV® R9140-B Lot # 2081000057 and the second test used Lot # 2002009604. PNNL has also performed ion exchange testing of Hanford tank waste and simulant using both lots of material. Fiskum et al. (2018) describe the simulant testing of Lot #2081000057, while Rovira et al. (2018) and Rovira et al. (2019a) describe the testing of Hanford tank waste with the same lot. Fiskum et al. (2019) describe extensive simulant testing at different bed heights in columns loaded with Lot # 2002009604, and Rovira et al. (2019b) describe the testing of Hanford tank waste. Recent testing was also performed with Lot # 2002009604 to assess the drying rate of CST media in a full-height column (Gauglitz et al. 2019).

The CST used in tested was pretreated prior to loading into the test vessels. The pretreatment generally involved rinsing the CST with aqueous fluids and storing it in sealed jars until it was used. The various pretreatment approaches are summarized below, since the approach varied depending on the test condition:

- For the CST in water test condition, the CST was rinsed with DI water, soaked in 0.1M NaOH for 1 hour, and stored under water until it was tested.

- For the CST in simulant test condition, the CST was rinsed in DI water, soaked in 0.1M NaOH for 1 hour, and stored under 0.1M NaOH until testing. The simulant was not in contact with the CST until the test vessels were loaded.

- For the wet free-drained CST test condition, the CST was rinsed in DI water, soaked in 0.1M NaOH for 1 hour, soaked in 3M NaOH overnight followed by a 1-hour 0.1M NaOH soak, and then soaked in DI water for 1 hour. The excess liquid was drained from the CST and the CST was sealed in a jar until the vessels were loaded for testing.

- For the dry CST test condition, the CST received the same treatment as the wet, free-drained CST, after which it was allowed to air dry on the lab bench until it reached a free-flowing state. After drying, the CST was stored in a jar until the vessels were loaded for testing.

For each condition, 10-samples were collected and then dried in an oven at 100°C until reaching a constant mass. The dry mass determination has historically been used for gas generation calculations to determine the amount of liquid in the system; however, in this case the results obtained using this method were inconsistent with other measurements that were conducted as a part of ion exchange testing. The moisture analysis results were used in the calculation instead as they appeared to be more consistent with what is expected. The moisture analysis results, when used as the basis for G-value calculations (see Section 4.6), provide more conservative (higher) values; this was deemed most appropriate for the ultimate use of the data, i.e., in CST column safety analyses.

The free-drained wet CST and dry CST samples from Test 1 and Test 2 were submitted for moisture analysis, which was conducted at 105°C using a moisture analyzer. The moisture analysis results can be found in Section 6.0 of this report. In addition, one replicate each of the rad and thermal wet CST and dry CST Test 2 samples were submitted for thermogravimetric analysis (TGA). The results of this analysis are FIO and can be found in Section 6 of this report.

4.2.3   Vessel Loading

Test vessels were prepared for loading by wrapping their exteriors with heat tape that included a thermocouple for heater and over-temperature control. Each vessel is approximately 60 mL in volume.

Vessels were loaded approximately half-full (30 mL) with liquid + CST (either water or simulant), wet CST, or dry CST. Thus, the 30 mL volume is the CST bed volume for each test condition. The loaded vessels were temporarily sparged with argon and capped. After all vessels had been prepared, the vessels were uncapped and installed in the testing apparatus.

4.3   Gamma Dose Calibration

A study and calibration of the gamma dose to the sample vessels was conducted prior to the start of testing. The study included three evaluation methodologies: air-equivalent ionization chamber measurements, radiochromic film irradiations, and MCNP modeling. The report of calibration is attached in its entirety as Appendix C of this report. The gamma dose calibration was specific to the source and vessels used in testing to provide an estimate (and the range of error) of the dose received by all of the samples in the radiolytic system.

4.4   Experiment Setup and Execution

The vessels were loaded into the testing apparatus and all electrical and gas line connections were made. The apparatus containing all reaction vessels was leak-tested prior to use. For testing, one apparatus for the non-rad (thermal) testing was located on the ground floor of the 318 Building, and one apparatus for the rad-exposure testing was located in the basement of the 318 Building.

Prior to starting the simulant experiments, the vapor pressure of the liquids was determined by connecting vessels containing simulant to the thermal system. The simulant liquid was refrigerated overnight prior to being loaded into duplicate vessels. The vessels were attached to the system, then they were purged and vented to atmospheric pressure with argon. The system was closed and the heater/controllers were turned on starting at a 25°C set point. The temperature and pressure were allowed to equilibrate and then the set point was increased at 10°C increments to just above the anticipated testing temperature. Testing was

conducted at 25°C with the exception of two vessels on each system during Test 2 which were held at 70°C. See Section 4.5 below for additional information. When the vessels reached maximum temperature, the heaters were turned off and the vessels were allowed to cool overnight with the data logger turned on. The cool-down temperature and pressure data were used to fit a curve to determine the vapor pressure function for the liquid. This function was used to correct the data for vapor pressure (see Section 4.6).

The rad-exposure apparatus, once connected and leak-checked, was lowered into the lead-shielded bunker. The bunker was then capped and the Co-60 source was transferred to the center of the bunker pneumatically and remotely. The transfer of the Co-60 source established time-zero (t_0) for the rad testing, and the thermal testing had a start time within a few hours of t_0. During the course of testing, temperatures and pressures were monitored daily during the week, and gas samples were taken approximately once a week. A more detailed description of how samples were collected is included below. Gas analysis was conducted on the gas mass spectrometer by PNNL's Analytical Support Operations organization in the Radiochemical Processing Laboratory (RPL) building. Analytes of interest were hydrogen, oxygen, methane, and nitrous oxide; however, other gases such as nitrogen, and hydrocarbons were also analyzed. After each gas sample, the test vessels were back-filled with argon and vented to atmospheric pressure through a bubbler.

At the conclusion of the test, the vessel heaters were turned off and the Co-60 source was transferred out of the bunker pneumatically. At that time, it was safe to remove the bunker shielding plug, and the reaction vessel apparatus was removed.

4.4.1   Gas Sampling

Each sampling event started with connecting 75-mL valved sampling bulbs to the gas sampling ports on the manifold. The bulb volumes were chosen to be larger than the system volume and were almost double the combined volume of the vessel, gas lines, and manifold. The bulbs were previously evacuated by the mass spectrometry lab to below 1×10^{-6} Torr. After the bulbs were connected to the manifold, the manifold vacuum valve was opened for each line, and the vacuum was turned on. The manifold was evacuated for approximately one hour prior to starting sampling. Gas samples were collected by closing the vacuum valve, opening the manifold sample valve and the valve on the sample bulb, and allowing the system to come to equilibrium. Then the manifold sample valve was closed, the sample bulb valve was closed, and the bulb was removed from the manifold. The process was repeated for each vessel. After sampling, the vessels were back-filled with argon and vented through a bubbler to reach atmospheric pressure.

4.5 Gas Generation Test Conditions

Table 4.3 summarizes the conditions tested in each of the two tests. Further detail about each of the tests is outlined below. Recall that Lot # 2081000057 was used in Test 1 and Lot # 2002009604 of CST was used in Test 2.

Table 4.3. Gas Generation Test Conditions Matrix

Test Condition	300 Mrad	900 Mrad
Laboratory-grade DI water + CST, ~25°C	Test 1	Not tested
Nominal 5.6M Na simulant (oxalate omitted) + CST, ~25°C	Test 1	Not tested
Nominal 5.6M Na simulant with 1% (w/w) TOC as HEDTA, ~25°C and 70°C	Test 2	Not tested
Free-drained, wet CST, ~25°C	Test 1	Test 2
Free-drained, air-dried CST, ~25°C	Test 1	Test 2

4.5.1 Test 1

Test 1 consisted of four separate conditions conducted in duplicate. The detailed experimental design for the rad system is found in Table 4.4 and the experimental design for the thermal system is found in Table 4.5. The conditions included CST in laboratory-grade DI water, CST in 5.6M Na simulant, free-drained wet CST, and free-drained air-dried CST. All four conditions were tested at ~25°C to a total dose of 323 Mrad. Test 1 was initiated on August 29, 2018, and concluded on September 21, 2018. The total accumulated time was just over 549 hours on the rad system and 545 hours on the thermal system. The average dose rate over the course of the experiment was 588 krad/hr.

Table 4.4. Test 1 Experimental Design – Rad System (shaded rows indicate duplicates)

Vessel #	System 1 (Rad System) – Gamma Experiments	Mass Liquid (g)	Dry CST Mass (g)
1-1	DI water + CST, 25°C	19.82	31.81
1-2	Free-drained wet CST, 25°C	16.68	26.77
1-3	Free-drained dry CST, 25°C	8.83	30.48
1-4	5.6M Na simulant + CST, 25°C	23.07	37.04
1-5	DI water + CST, 25°C, duplicate	19.99	32.09
1-6	Free-drained wet CST, 25°C, duplicate	16.99	27.27
1-7	Free-drained dry CST, 25°C, duplicate	8.21	28.37
1-8	5.6M Na simulant + CST, 25°C, duplicate	20.26	32.52

Table 4.5. Test 1 Experimental Design – Thermal System (shaded rows indicate duplicates)

Vessel #	System 2 (Thermal System) – Thermal-only Experiments	Mass Liquid (g)	Dry CST Mass (g)
2-1	DI water + CST, 25°C	19.06	30.61
2-2	Free-drained wet CST, 25°C	19.18	30.79
2-3	Free-drained dry CST, 25°C	8.67	29.97
2-4	5.6M Na simulant + CST, 25°C	22.99	36.91
2-5	DI water + CST, 25°C, duplicate	20.64	33.15
2-6	Free-drained wet CST, 25°C, duplicate	20.27	32.55
2-7	Free-drained dry CST, 25°C, duplicate	8.14	28.12
2-8	5.6M Na simulant + CST, 25°C, duplicate	21.07	33.83

Three gas samplings took place over the course of the experiment, on September 5 (~161 hr), 12 (331 hr), and 21 (545 hr), 2018. The gas samples were delivered to the gas mass spectrometry laboratory in the PNNL RPL building for analysis. After the final gas sampling, the Co-60 source was removed from the gamma bunker, and a fresh argon gas atmosphere was introduced into each vessel. The vessels were removed from the thermal system on September 21, 2018, and from the rad system on September 24, 2018, and were transferred to RPL for unloading and examination of the vessel contents. The thermal system vessels were unloaded on September 21, 2018, and the rad system vessels were unloaded on September 25, 2018.

4.5.2　Test 2

The Test 2 conditions included CST in 5.6M Na simulant with 1% (w/w) TOC as HEDTA at 25°C and 70°C to a total dose of 298 Mrad, free-drained wet CST at 25°C, and free-drained air-dried CST at 25°C, both of which were tested to a total accumulated dose of 908 Mrad. The experimental design for the rad system can be found in Table 4.6 and the experimental design for the thermal system can be found in Table 4.7. Test 2 was initiated on January 9, 2019. The heaters controlling temperature of the simulant vessels were turned off and the vessels were vented to the bubbler starting on January 31, 2019. The test concluded on March 18, 2019. For the simulant vessels, the total accumulated time was just over 528 hours on the rad system with an average dose rate of 561 krad/hr and 524.5 hours on the thermal system. The remainder of the vessels had a total accumulated time of just over 1,630 hours on the rad system with an average dose rate of 556 krad/hr and almost 1,627 hours on the thermal system.

Table 4.6. Test 2 Experimental Design – Rad System (shaded rows indicate duplicates)

Vessel #	System 1 (Rad System) - Gamma Experiments	Mass Liquid (g)	Dry CST Mass (g)
1-1	Wet CST, 25°C	20.92	31.96
1-2	5.6M Na simulant w/ TOC + CST, 25°C	22.50	34.37
1-3	Dry CST, 25°C	3.44	27.52
1-4	5.6M Na simulant w/ TOC + CST, 70°C	21.47	32.78
1-5	Wet CST, 25°C, duplicate	20.76	31.70
1-6	5.6M Na simulant w/ TOC + CST, 25°C, duplicate	21.34	32.60
1-7	Dry CST, 25°C, duplicate	3.56	28.45
1-8	5.6M Na simulant w/ TOC + CST, 70°C, duplicate	21.04	32.14

Table 4.7. Test 2 Experimental Design – Thermal System (shaded rows indicate duplicates)

Vessel #	System 2 (Thermal System) – Thermal-only Experiments	Mass Liquid (g)	Dry CST Mass (g)
2-1	Wet CST, 25°C	20.43	31.19
2-2	5.6M Na simulant w/ TOC + CST, 25°C	20.48	31.27
2-3	Dry CST, 25°C	3.56	28.43
2-4	5.6M Na simulant w/ TOC + CST, 70°C	19.97	30.51
2-5	Wet CST, 25°C, duplicate	20.53	31.36
2-6	5.6M Na simulant w/ TOC + CST, 25°C, duplicate	20.93	31.97
2-7	Dry CST, 25°C, duplicate	3.53	28.22
2-8	5.6M Na simulant w/ TOC + CST, 70°C, duplicate	23.15	35.36

A total of 10 gas sampling events took place over the course of the experiment; a summary of the events is provided in Table 4.8. The gas samples were delivered to the gas mass spectrometry laboratory in the PNNL RPL building for analysis. After the final gas sampling, the source was removed from the gamma bunker, and a fresh argon gas atmosphere was introduced to each vessel. The vessels were removed from the thermal system on March 18, 2019, and from the rad system on March 19, 2019, and were transferred

to RPL for unloading and examination of the vessel contents. All of the vessels were unloaded on March 20, 2019.

Table 4.8. Summary of Test 2 Gas Sampling Events

Sample Date	Run Time (hr)	Vessels Sampled	Total Samples Collected
January 14, 2019	126.75	All	16
January 18, 2019	215.58	Simulant vessels on the rad system	4
January 23, 2019	335.67	All	16
January 31, 2019	528.08	All	16
February 7, 2019	695.83	Wet CST and dry CST vessels on both systems	8
February 15, 2019	890.25	Wet CST and dry CST vessels on both systems	8
February 21, 2019	1036.17	Wet CST and dry CST vessels on both systems	8
February 28, 2019	1202.50	Wet CST and dry CST vessels on both systems	8
March 7, 2019	1366.92	Wet CST and dry CST vessels on both systems	8
March 18, 2019	1630.33	Wet CST and dry CST vessels on both systems	8

4.6 Data Analysis

The analysis approach set forth in previous work by Colburn et al. (2018) was used for the test data of the current work: the temperatures, pressures, and gas analysis data were analyzed to determine the gas generation rates under the different process conditions. Briefly, the ideal gas law was used to determine the moles of gas present in each system, based on the known system volume and temperature and pressure measurements. The moles calculation was broken up into different portions of the system using the temperature measurements of each portion, where the portions are (1) the manifold to the pressure transducer, (2) the pressure transducer to the top of the vessel, and (3) the vessel headspace. In general, the vessel headspace volume is approximately 90% of the total system volume. To accurately determine the number of moles of dry gas generated, the vapor pressure of the relevant liquid was determined and subtracted from the pressure measurement prior to the moles calculation. Gas mass spectrometry was used to determine the composition (mole %) of hydrogen and the other gases generated. By combining the total moles measurement with the mole % composition, the moles of hydrogen, oxygen, methane, and nitrous oxide were determined. The generation rate of each gas can be determined in moles per kg of liquid per day using the run time and mass of liquid in the system. The precision of the measurements was assessed by comparing the experimental duplicates.

The G-values of hydrogen, oxygen, methane, and nitrous oxide generated within the experiment can be calculated by the following equation, from the moles of gas formed and the calculated absorbed dose.

$$G\left(H_2\right) = \frac{\text{number of } H_2 \text{ molecules formed}}{100 \text{ eV absorbed dose}}$$

It was assumed that the gas generation occurred overwhelmingly within the liquid phase, and therefore the absorbed dose used for purposes of G-value calculation is the dose absorbed by the liquid phase alone. The mass of liquid in the system is derived from the moisture analysis measurements of the CST. As mentioned in Section 4.2.2, the use of moisture analysis data to calculate the liquid phase basis produces more conservative (larger) G-values. G-values for other gas components were determined in a similar way.

5.0 Gas Generation Testing Experimental Design and Results

A total of two gas generation tests of CST were conducted. In the first test, four different TSCR operating and storage conditions were tested in duplicate in both the rad and thermal systems for a total of 16 vessels. Due to resource limitations, liquid-only controls were not included in this series of tests as they were in previous ion exchange media testing (Colburn et al. 2018). The liquid-only controls included in the previous testing allowed a direct observation of the contribution of the ion exchange medium on gas generation compared to the liquid-only control. Without these controls, the contribution of the CST cannot be directly deduced, but rather can be inferred based on the results observed in the previous testing. The thermal system tests were conducted for approximately the same periods of time as the corresponding rad system tests. Note that the results are summarized in this section by process condition and not by test. The results of Test 1 prompted a change of the work scope to include an extended irradiation to 900 Mrad of the TSCR storage condition CST (free-drained wet CST and free-drained dry CST).

Gas composition measurements based on mass spectral results for each gas sampling event are given in Appendix A. Based on these measurements, the total moles of hydrogen, oxygen, methane, and nitrous oxide were determined at each sampling event using system volume, temperature, pressure, and vapor pressure. Gas generation of CST in water is summarized in Section 5.1. Gas generation of CST in simulant with and without additional TOC is summarized in Section 5.2. Finally, the gas generation of the free-drained CST material simulating TSCR column storage conditions is summarized in Section 5.3.

As a comparison, the previous published G-values for CST and similar media are presented in Table 5.1.

Table 5.1. Previous Gas Generation Study G-values

Reference	G-Value	Description
Bibler et al. 1998	0.2	63% water/37% CST, 35°C 4×10^5 Rad/hr for <150 hours
Walker et al. 1999	0.25 (G_{tot})	Savannah River Site Tank 44F w/ CST, no reported dose rate.
Walker et al. 1999	0.11 (G_{tot})	High nitrate solution /IE-911 slurry 1 Mrad/hr, 7 days – 168 Mrad total dose
Walker et al. 1999	0.07 (G_{tot})	High OH /IE-911 slurry 1 Mrad/hr, 7 days – 168 Mrad total dose
Swyler and Barletta 1983	0.25 (G_{H2+O2})	Fast e-irradiation, 75°C, 6.5×10^8 Rad/hr. Three Mile Island, 50% water /IE-95 zeolite

5.1 CST in Water

The gas generation of CST in water was tested in Test 1 with an average dose rate of 588 krad/hr for a total dose of 323 Mrad over 23 days. The observed cumulative G-values for hydrogen, methane, oxygen, and nitrous oxide in the CST in water condition are listed in Table 5.2. The G-values have been corrected for thermal generation although the observed thermal generation is very small. Hydrogen gas generation from CST in water is shown in Figure 5.1 for the thermal + irradiation experiment. Oxygen gas generation from CST in water is shown in Figure 5.2 for the thermal + irradiation experiment. Note that initially little to no oxygen was observed, but over the course of the experiment the oxygen generation was observed to increase. Early oxygen generation may be masked by the data corrections that were made for air in-leakage; however, in most cases, the air in-leakage was small.

Table 5.2. Observed cumulative G-values (molecules/100 eV absorbed dose) for CST in water, 25°C, total dose 323 Mrad

Time (hr)	$G(H_2)$	$G(CH_4)$	$G(O_2)$	$G(N_2O)$
162.50	0.2798	0.0013	0.0013	0.0006
335.08	0.2967	0.0008	0.0351	0.0004
549.33	0.3132	0.0005	0.0707	0.0003
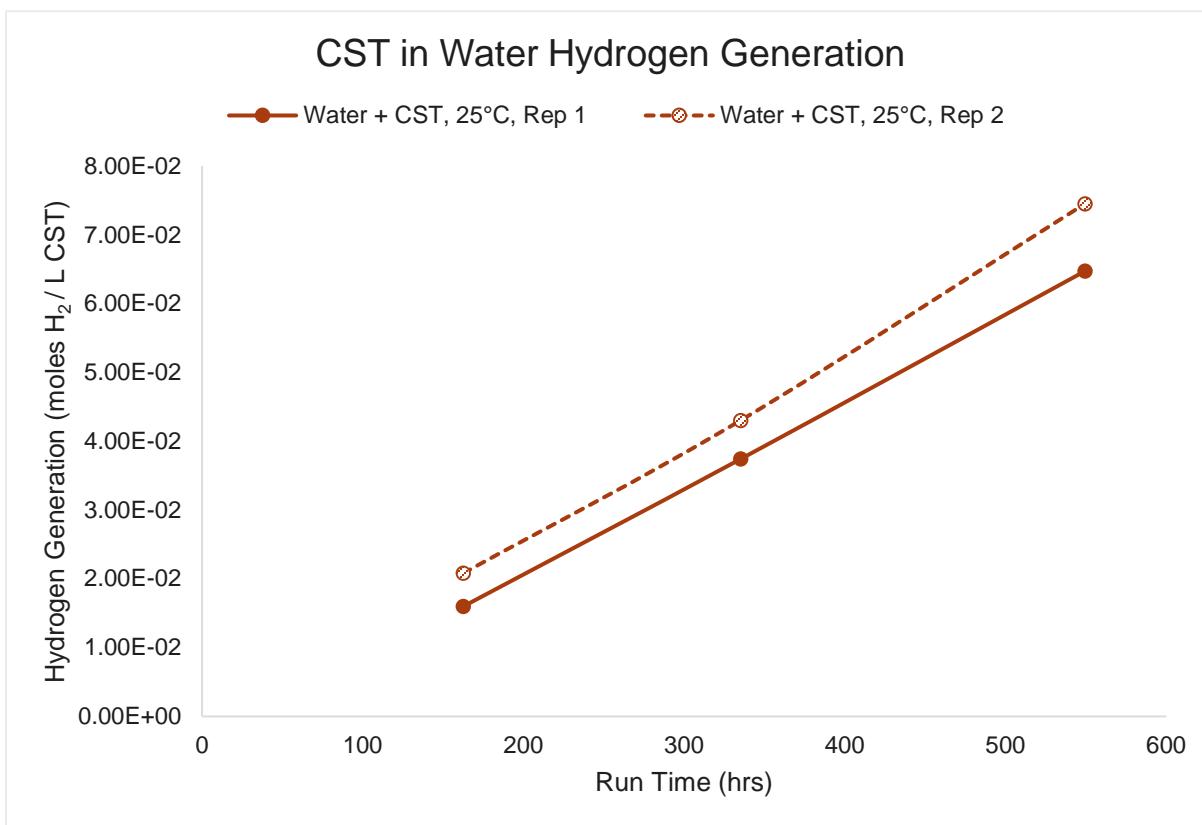
Figure 5.1. Cumulative hydrogen generation of CST in water at 25°C. The total accumulated dose was 323 Mrad.
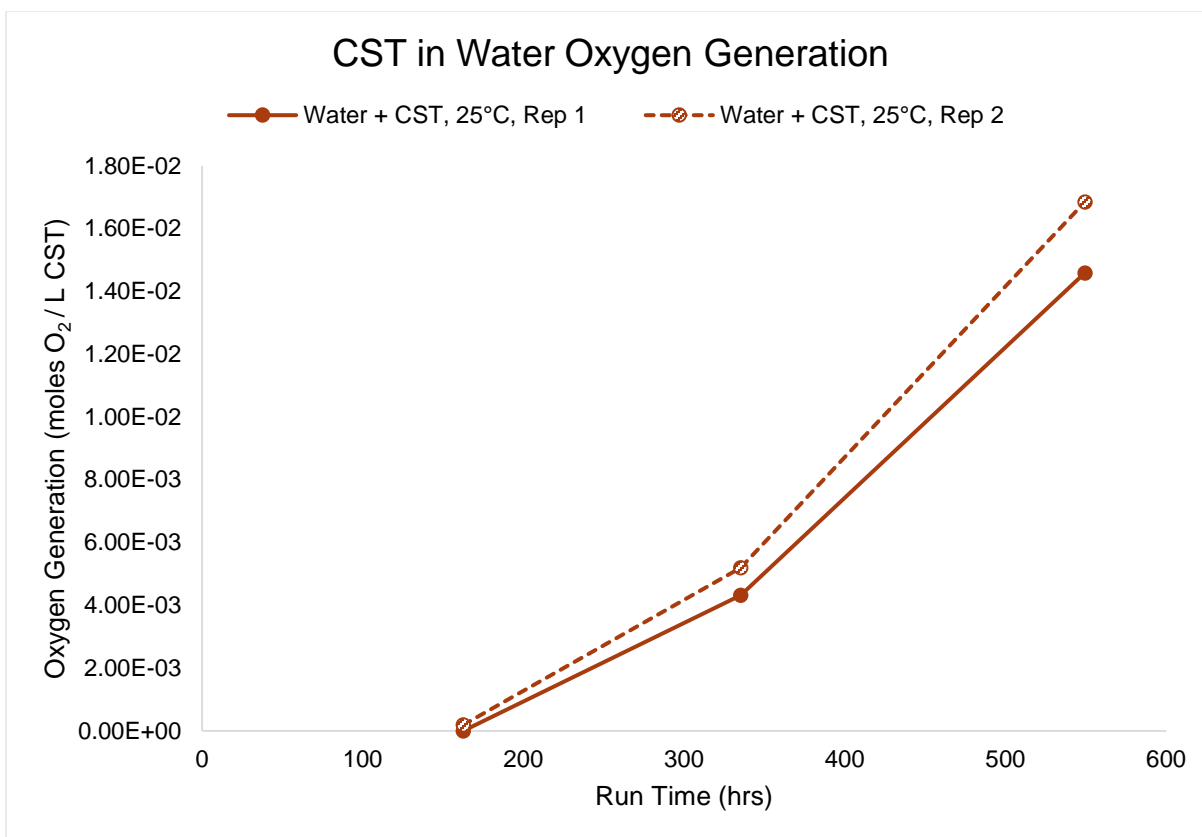
Figure 5.2. Cumulative oxygen generation of CST in water at 25°C. The total accumulated dose was 323 Mrad.

5.2 CST in Simulant

The gas generation of CST in simulant was tested as summarized in Table 4.3. The G-values for hydrogen, oxygen, and nitrous oxide are found in Table 5.3, Table 5.4, and Table 5.5, respectively. Methane generation was negligible. The simulant without TOC generated a significant amount of oxygen, while the simulant with TOC did not. The opposite case is true for the generation of nitrous oxide. Figure 5.3, Figure 5.4, and Figure 5.5 show, respectively, the gas generation of hydrogen, oxygen, and nitrous oxide for all CST in simulant cases. Note that the actual nitrous oxide G-values may be slightly larger than those reported since the trace thermal generation of nitrous oxide observed was not distinguishable from carbon dioxide. The mass spectrometry data analysis assumed that all of the gas corresponding to the shared *m/z* 44 peak was nitrous oxide.

Table 5.3. Observed cumulative $G(H_2)$-values for CST in simulant

Run Time (hr)	Simulant w/o TOC (25°C)	Run Time (hr)	Simulant w/ TOC (25°C)	Simulant w/ TOC (70°C)
162.50	0.0680	126.75	0.0840	0.1199
335.08	0.0710	215.58	0.0889	0.1161
549.33	0.0732	335.67	0.0950	0.1190
---	---	528.08	0.1035	0.1210
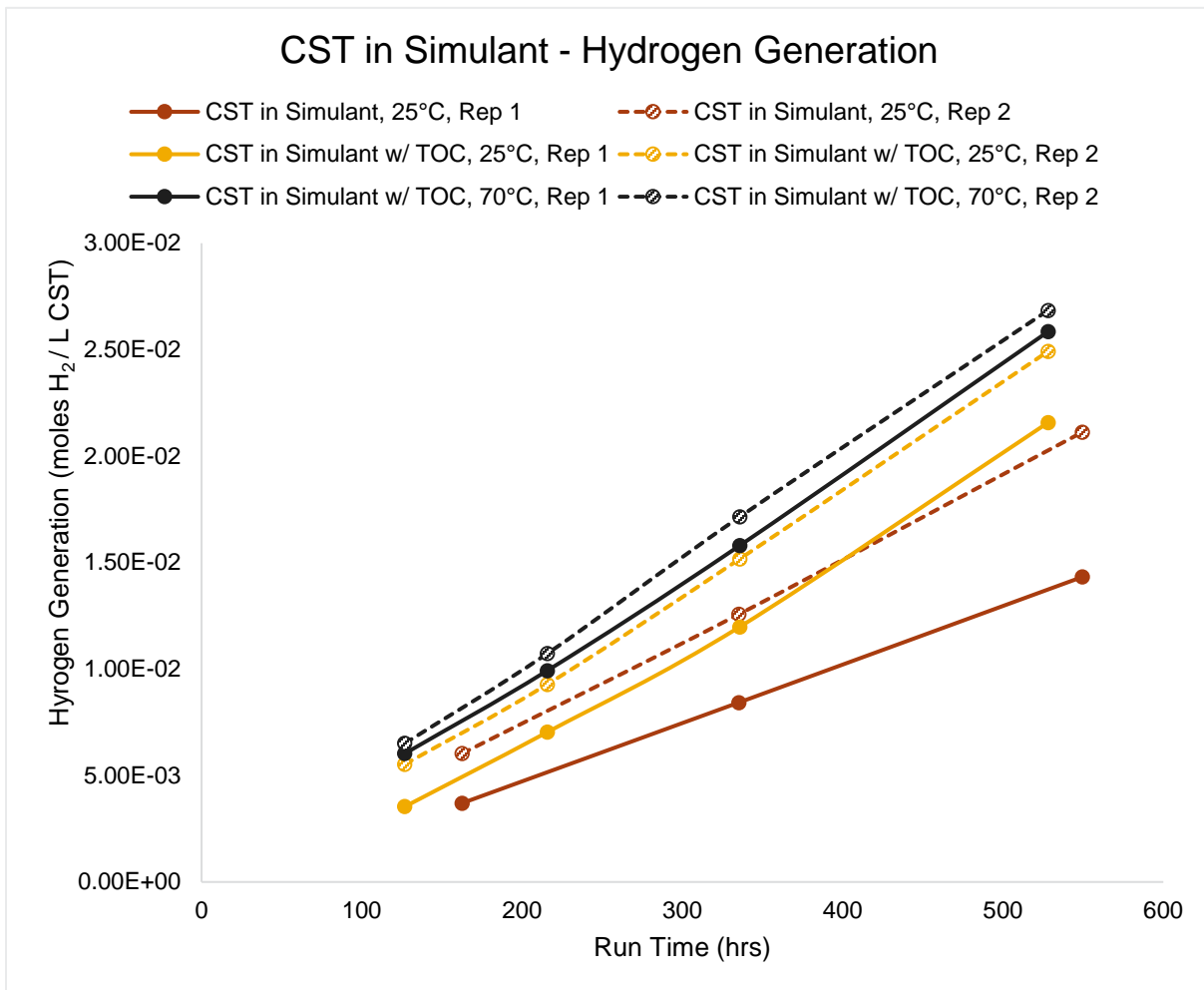
Figure 5.3. Cumulative hydrogen generation for all CST in simulant tests.

Table 5.4. Observed cumulative $G(O_2)$-values for CST in simulant

Run Time (hr)	Simulant w/o TOC (25°C)	Run Time (hr)	Simulant w/ TOC (25°C)	Simulant w/ TOC (70°C)
162.50	0.1252	126.75	No O_2 observed	No O_2 observed
335.08	0.1418	215.58	No O_2 observed	No O_2 observed
549.33	0.1464	335.67	No O_2 observed	No O_2 observed
---	---	528.08	0.0046	0.0044
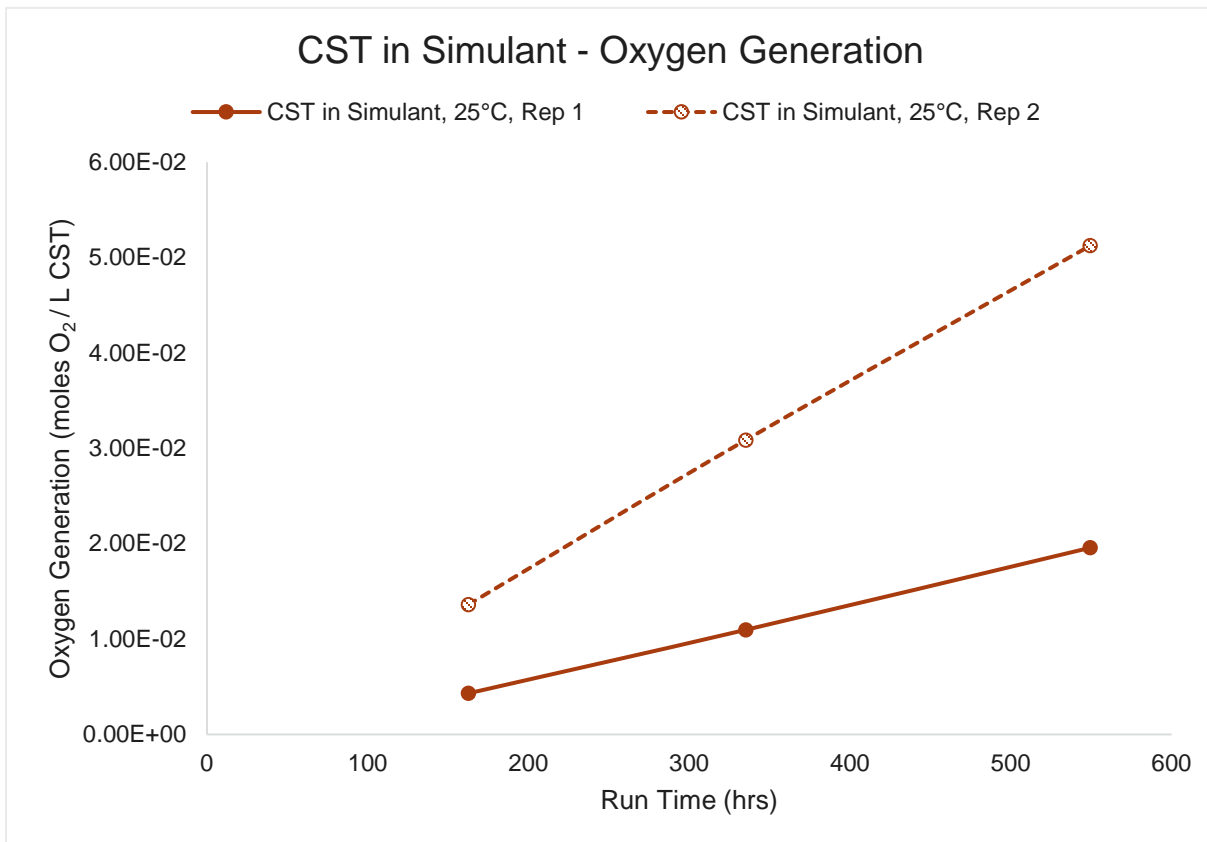
Figure 5.4. Cumulative oxygen generation from the CST in 5.6M Na simulant without TOC.

Table 5.5. Observed cumulative G(N$_2$O)-values for CST in simulant

Run Time (hr)	Simulant w/o TOC (25°C)	Run Time (hr)	Simulant w/ TOC (25°C)	Simulant w/ TOC (70°C)
162.50	0.0005	126.75	0.3917	0.4373
335.08	0.0008	215.58	0.3146	0.3072
549.33	0.0007	335.67	0.2313	0.2121
---	---	528.08	0.1671	0.1592
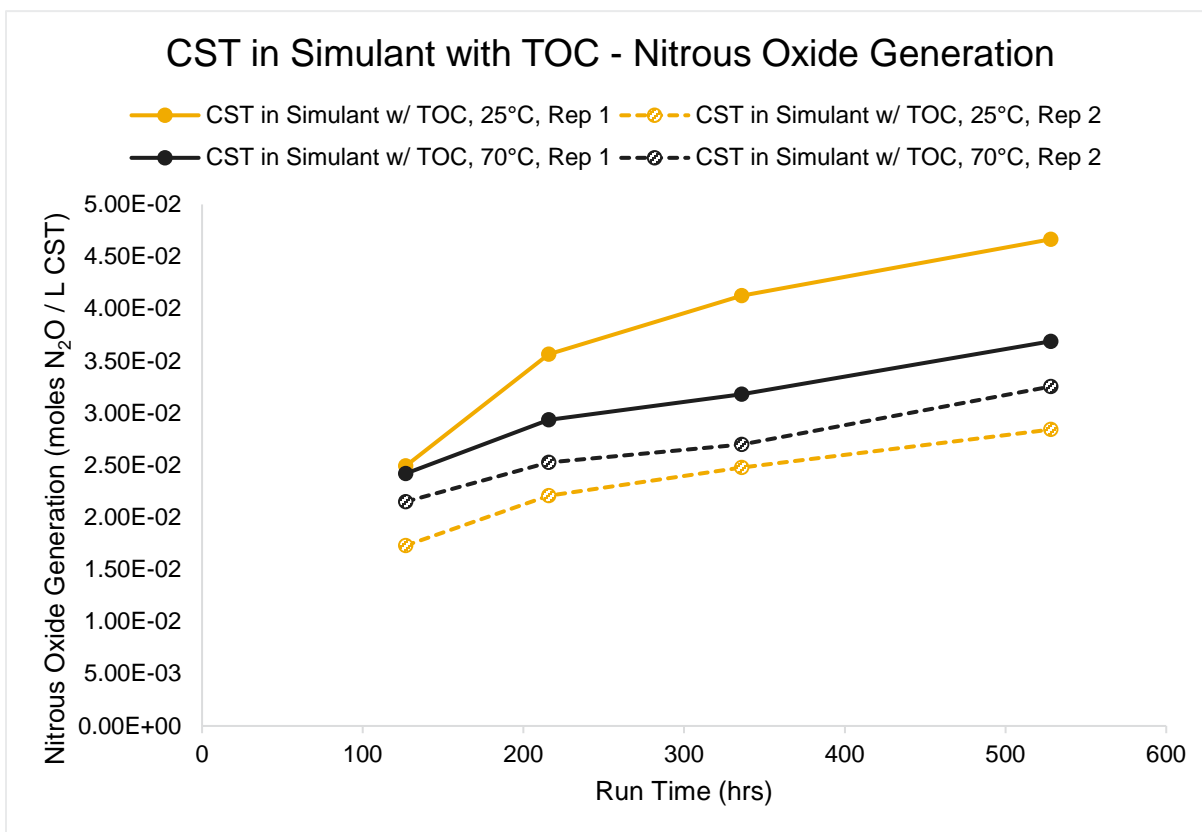
Figure 5.5. Cumulative nitrous oxide generation per liter of CST for CST in simulant with 1% (w/w) TOC as HEDTA.

5.3 Storage Condition CST

The cesium loaded onto the CST is not readily eluted from the column. Therefore, the CST material will be used once and the fully loaded columns will require storage prior to final disposition. The current proposed operating condition for a loaded column is to displace the feed with 0.1M NaOH, followed by a water rinse. The water will then be displaced by air and will continue to be air dried past the point that the

U.S. Environmental Protection Agency Paint Filter Liquids Test[1] is passed (see Gauglitz et al. 2019). At this point, the column will be transported and stored on an interim storage pad. As a result, some level of moisture is anticipated to remain in the CST bed. The corresponding radioactivity can lead to radiolytic gas generation from the CST in storage. To that end, the gas generation of CST was tested with free-drained wet CST and lab-equilibrated "dry" CST that had been free-drained and allowed to air dry on the bench until it was free flowing. These conditions were tested in duplicate with two different lots of CST and for two different irradiation end-points of 300 Mrad and 900 Mrad. The results for the wet and dry materials are highlighted in Sections 5.3.1 and 5.3.2, respectively.

5.3.1   Wet CST

Free-drained wet CST produced hydrogen and oxygen under radiolytic conditions. Methane and nitrous oxide were not observed above trace amounts. Table 5.6 presents the observed $G(H_2)$-values and $G(O_2)$-values for wet CST in both Tests 1 and 2. The G-values have been corrected for thermal generation. In the case of oxygen: for the early data points, the thermal generation was greater than the radiolytic generation—although small in both cases and likely within the experimental error—which accounted for the negative values. Note that the G-values for Test 1 were much larger than those observed in Test 2. Although the moisture levels are similar, it has been documented that the two lots of CST behave differently in their ion exchange behavior, indicating that the two lots are different; see Fiskum et al. (2018) and Fiskum et al. (2019). The difference between the two lots is significant enough that further examination of additional lots of CST material to understand the gas generation behavior may be warranted. Figure 5.6 shows the cumulative hydrogen generation for wet CST observed in both tests, while Figure 5.7 shows the cumulative oxygen generation observed.

Table 5.6. Observed cumulative $G(H_2)$ and $G(O_2)$ for free-drained wet CST

Test 1 – CST Lot # 2081000057 549 hours, 323 Mrad total			Test #2 – CST Lot # 2002009604 1630 hours, 908 Mrad		
Run Time (hr)	$G(H_2)$ (molecules/100 eV)	$G(O_2)$ (molecules/100 eV)	Run Time (hr)	$G(H_2)$ (molecules/100 eV)	$G(O_2)$ (molecules/100 eV)
162.5	0.1069	-0.0002	126.75	0.0159	-0.0027
335.08	0.1165	0.0062	335.67	0.0154	-0.0011
549.33	0.1259	0.0194	528.08	0.0163	0.0003
---	---	---	695.83	0.0166	0.0012
---	---	---	890.25	0.0172	0.0020
---	---	---	1036.17	0.0176	0.0025
---	---	---	1202.50	0.0180	0.0030
---	---	---	1366.92	0.0183	0.0034
---	---	---	1630.33	0.0191	0.0040

---

[1]   The Paint Filter Liquids Test, described in EPA Method 9095B, Rev. 2 (November 2004), *Paint Filter Liquids Test*, is a method for determining the presence of free liquids in a representative sample of waste, used to determine compliance with Federal regulations governing hazardous waste transportation and storage.
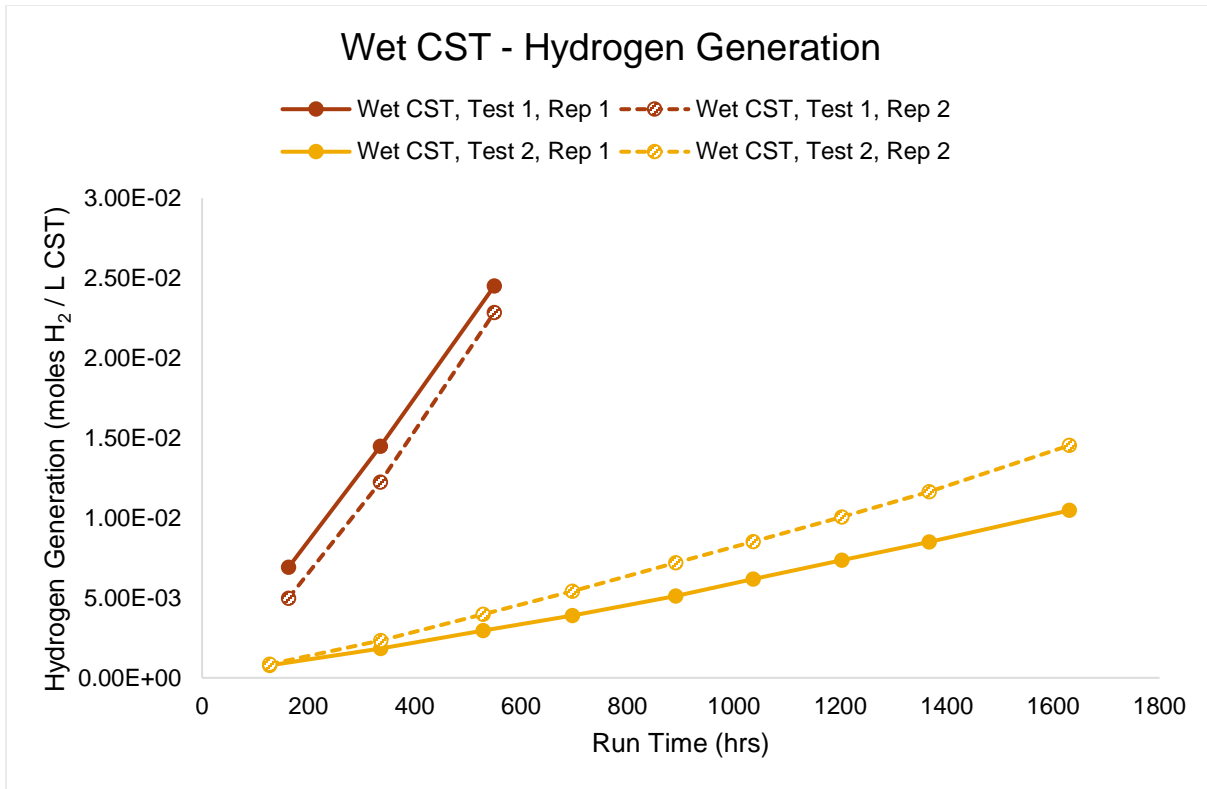
Figure 5.6. Cumulative hydrogen generation of wet CST for Test 1 and Test 2.
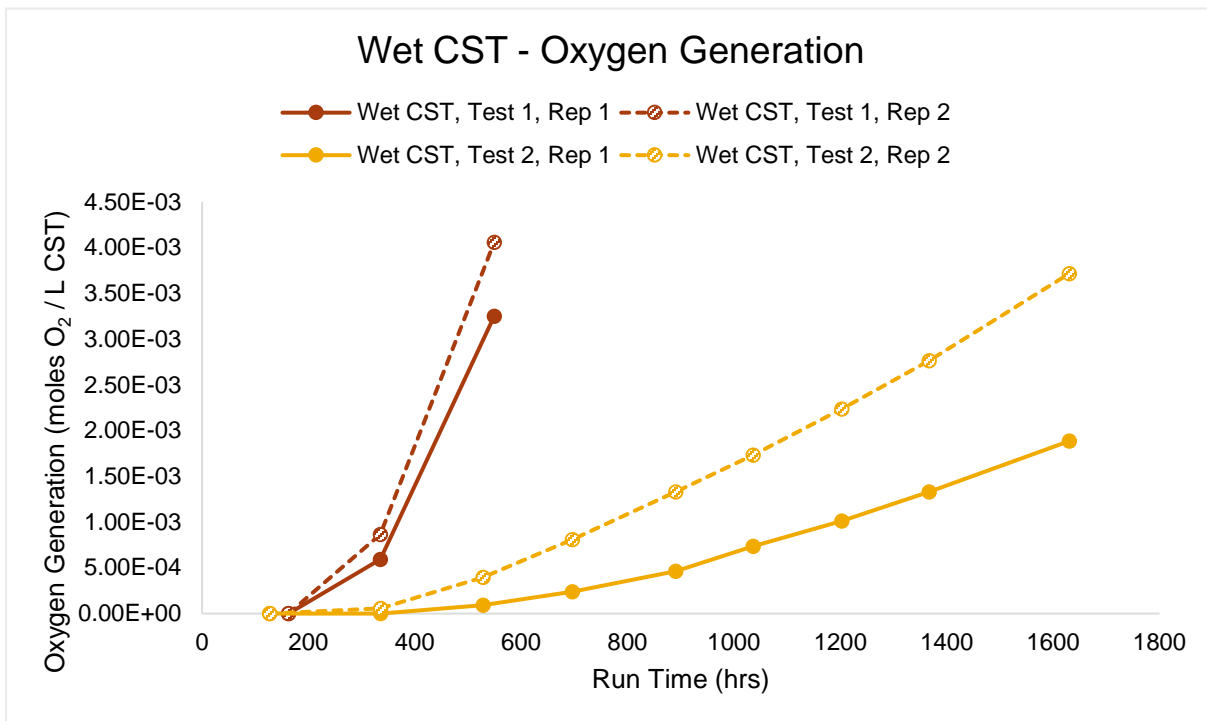
Figure 5.7. Cumulative oxygen generation of wet CST for Test 1 and Test 2.

5.3.2   Dry CST

Free-drained dry CST produced hydrogen and oxygen under radiolytic conditions, but no methane or nitrous oxide in Test 1. In Test 2, the CST produced hydrogen, along with trace amounts of methane and nitrous oxide (G-values of 0.0003 and 0.0001, respectively). Table 5.7 presents the observed $G(H_2)$ and $G(O_2)$-values for dry CST in both Test 1 and Test 2. The G-values have been corrected for thermal generation. In the case of oxygen, the corrected generation rate was negligible for all the samples collected in Test 2. Note that the $G(H_2)$-values for Test 1 were larger than those observed in Test 2. Figure 5.8 shows the cumulative hydrogen generation for dry CST observed in both tests, while Figure 5.9 shows the cumulative oxygen generation observed.

Table 5.7. Observed cumulative $G(H_2)$ and $G(O_2)$ for free-drained dry CST

Test 1 – CST Lot # 2081000057 549 Hours, 323 Mrad Total			Test #2 – CST Lot # 2002009604 1,630 Hours, 908 Mrad		
Run Time (hr)	$G(H_2)$ (molecules/100 eV)	$G(O_2)$ (molecules/100 eV)	Run Time (hr)	$G(H_2)$ (molecules/100 eV)	$G(O_2)$ (molecules/100 eV)
162.5	0.3133	0.0067	126.75	0.0991	No O_2 observed
335.08	0.3212	0.0398	335.67	0.1033	No O_2 observed
549.33	0.3291	0.0689	528.08	0.1032	No O_2 observed
---	---	---	695.83	0.1019	No O_2 observed
---	---	---	890.25	0.0984	No O_2 observed
---	---	---	1036.17	0.0977	No O_2 observed
---	---	---	1202.50	0.0955	No O_2 observed
---	---	---	1366.92	0.0939	No O_2 observed
---	---	---	1630.33	0.0894	No O_2 observed
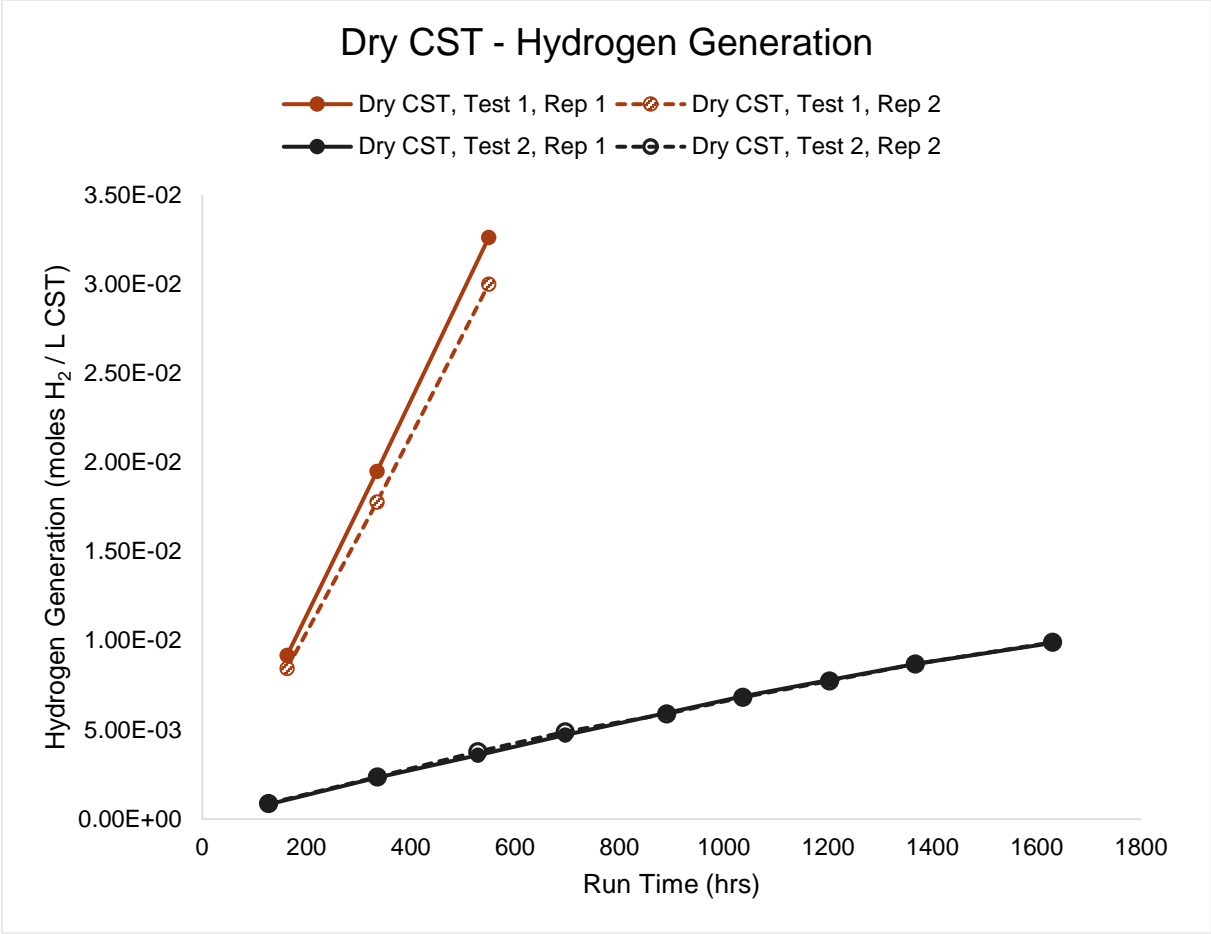
Figure 5.8. Cumulative hydrogen generation from free-drained dry CST for Test 1 and Test 2.
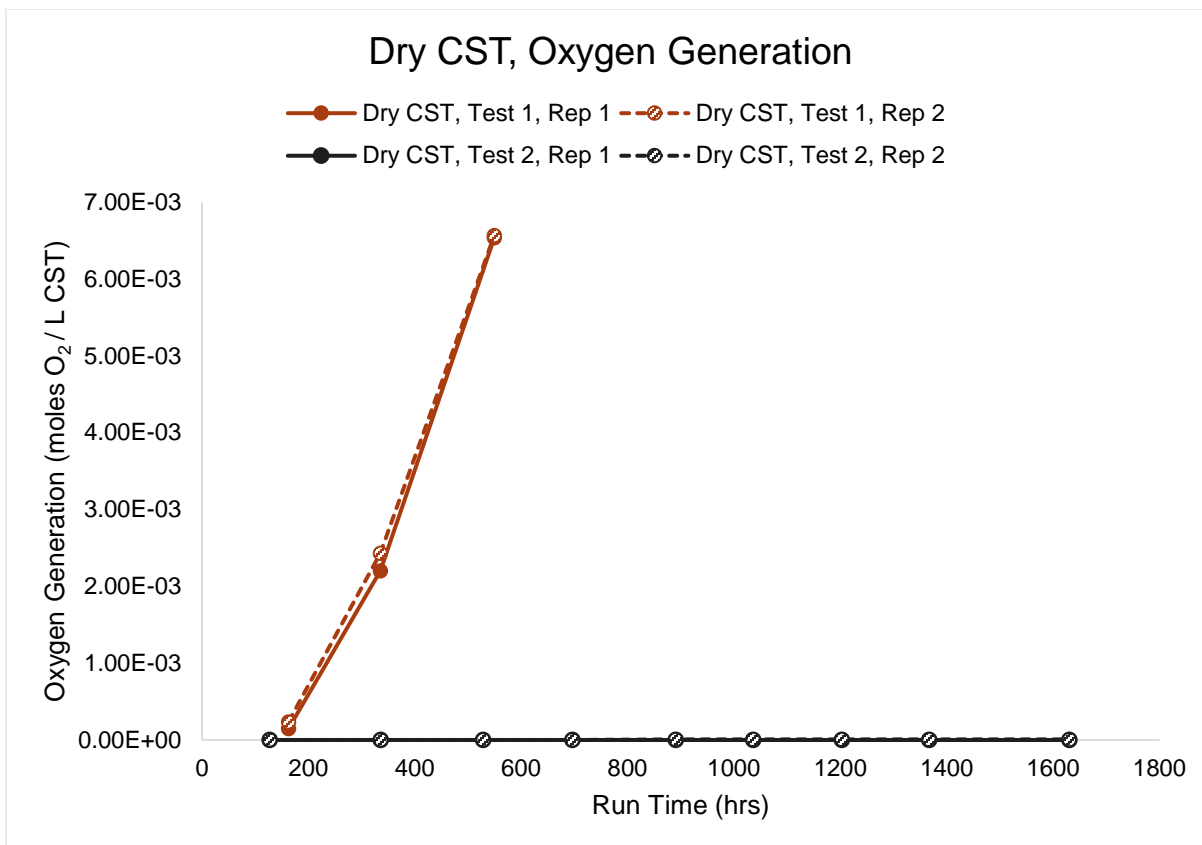
Figure 5.9. Cumulative oxygen generation from free-drained dry CST for Test 1 and Test 2.

5.4 Recap of CST Conditions Tested

The gas generation of CST was tested under different TSCR operating and column storage conditions. Of the operating conditions, CST in water returned the largest $G(H_2)$-value, while CST in 5.6M Na simulant returned the largest $G(O_2)$-value. Of the storage conditions, the first lot of CST tested (Lot # 2081000057) returned the largest $G(H_2)$-value for the dry CST, and that lot had $G(O_2)$-values that were approximately a factor of five smaller than the $G(H_2)$ values for both the wet and dry CST. By comparison, the second lot of CST (Lot # 2002009604) tested under storage conditions had significantly smaller G-values for both hydrogen and oxygen. Generation of methane and nitrous oxide was at trace levels (if observed) except in the case of nitrous oxide generation in the 5.6M Na simulant with TOC. Table 5.8 provides a summary of the final cumulative G-values observed in the CST gas generation testing. In some cases, the maximum observed G-values were not at the completion of testing. In order to capture this behavior, the maximum G-values are listed in Table 5.9. Comparison plots of the hydrogen generation and oxygen generation of the various gas generation tests are shown in Figure 5.10 and Figure 5.11, respectively.

Table 5.8. Final cumulative G-values. All test conditions at 25°C except where noted.

Test Condition	$G(H_2)$ – molecules H_2/100 eV	$G(CH_4)$ – molecules CH_4/100 eV	$G(O_2)$ – molecules O_2/100 eV	$G(N_2O)$ – molecules N_2O/100 eV
CST in water	0.3132	0.0005	0.0707	0.0003
CST in 5.6M Na simulant	0.0732	3.52×10^{-5}	0.1464	0.0007
CST in 5.6M Na simulant w/ TOC	0.1035	4.53×10^{-5}	0.0046	0.1671
CST in 5.6M Na simulant w/ TOC, 70°C	0.1210	3.94×10^{-5}	0.0044	0.1592
Wet CST – Test 1	0.1259	No CH_4 observed	0.0194	No N_2O observed
Wet CST – Test 2	0.0191	9.47×10^{-6}	0.0040	No N_2O observed
Dry CST – Test 1	0.3291	No CH_4 observed	0.0689	0.0004
Dry CST – Test 2	0.0894	0.0003	No O_2 observed	9.1×10^{-5}

Table 5.9. Maximum observed G-values. All test conditions at 25°C except where noted.

Test Condition	$G(H_2)$ – molecules H_2/100 eV	$G(CH_4)$ – molecules CH_4/100 eV	$G(O_2)$ – molecules O_2/100 eV	$G(N_2O)$ – molecules N_2O/100 eV
CST in water	0.3132	0.0013	0.0707	0.0006
CST in 5.6M Na simulant	0.0732	3.52×10^{-5}	0.1464	0.0008
CST in 5.6M Na simulant w/ TOC	0.1035	4.53×10^{-5}	0.0046	0.3917
CST in 5.6M Na simulant w/ TOC, 70°C	0.1210	3.94×10^{-5}	0.0044	0.4373
Wet CST – Test 1	0.1259	No CH_4 observed	0.0194	No N_2O observed
Wet CST – Test 2	0.0191	1.85×10^{-5}	0.0040	No N_2O observed
Dry CST – Test 1	0.3291	No CH_4 observed	0.0689	0.0005
Dry CST – Test 2	0.1033	0.0003	No O_2 observed	0.0005
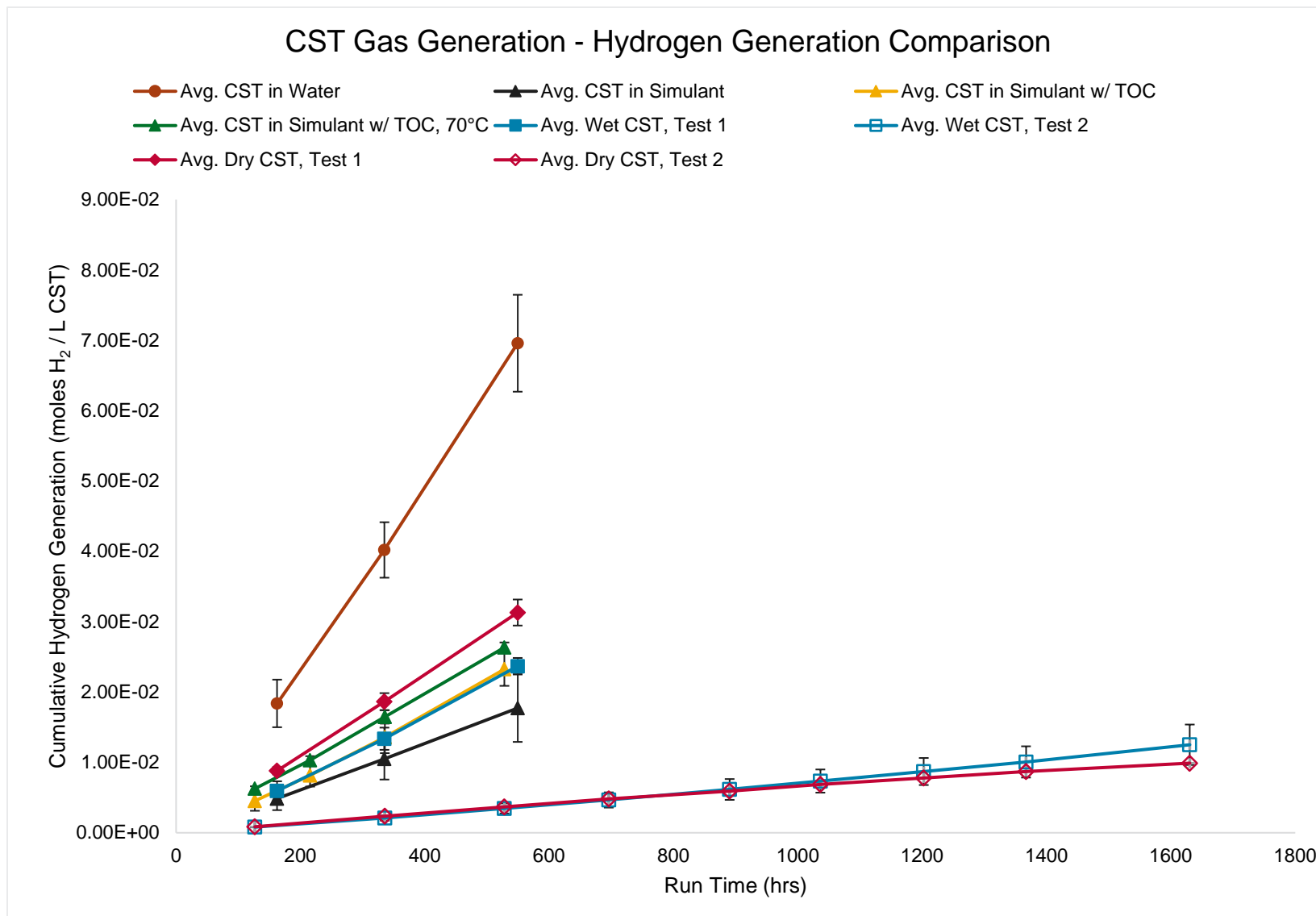
Figure 5.10. Average cumulative hydrogen generation for each test condition. Error bars indicate one standard deviation.
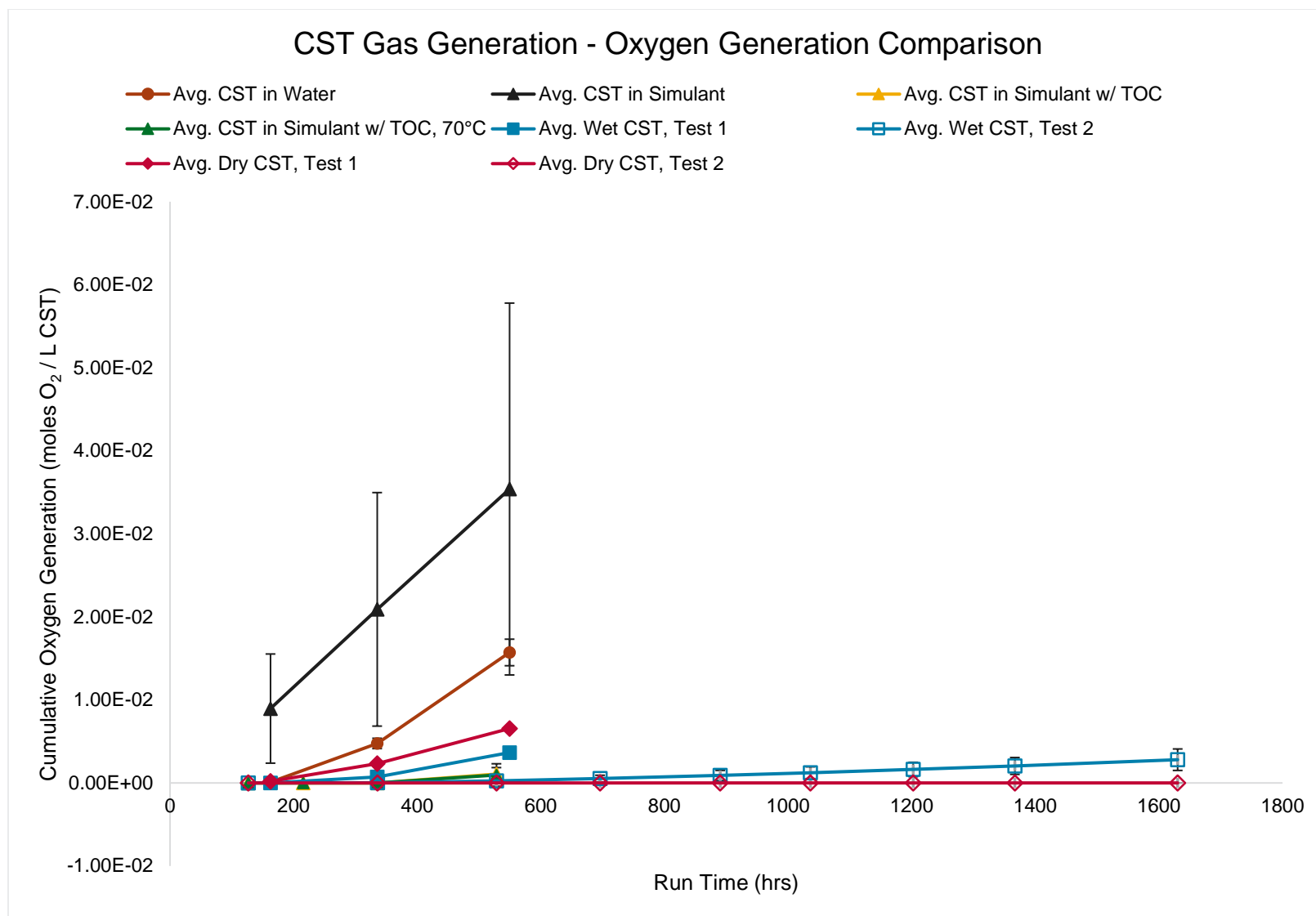
Figure 5.11. Average cumulative oxygen generation for the test conditions. Error bars indicate one standard deviation.

6.0 CST Moisture Analysis and TGA Analysis Results

Samples of the prepared CST were submitted for moisture analysis after preparation for both tests. In addition, the as-received Test 2 CST was analyzed along with the post-test wet and dry CST after Test 2. The moisture analysis data collected at 105°C (with the exception of the Test 2 pre-test samples[1]) are presented in Table 6.1. The as-received CST and post-test samples from Test 2 were also analyzed by TGA as a FIO analysis. The TGA moisture content results are presented in Table 6.2 compared to the moisture analyzer results. Note that the TGA data, initially measured as dry content (in wt%), were inverted to present the data in terms of moisture content via the expression: moisture content = 100 – dry content.

Table 6.1. CST moisture analysis results.

Sample	As-received CST	Wet CST	Dry CST
CST-01 Lot #2002009604 (Test 2 Lot)	5.48%	--	--
Test 1	--	38.38%	22.45%
Test 2[(a)]	--	39.57%	11.12%
Test 2, post-test, rad	--	39.32%	17.12%
Test 2, post-test, thermal	--	40.03%	9.24%
(a) Note that the moisture content of these samples was measured at 160°C instead of 105°C.			

Table 6.2. Results from thermogravimetric analysis (for information only) of CST compared to the moisture analyzer.

Measurement Data	SRNL Data (King et al. 2018b)	PNNL As-Received (CST-01)	Post-test Rad 1-1 (Wet CST)	Post-test Thermal 2-1 (Wet CST)	Post-test Rad 1-3 (Dry CST)	Post-test Thermal 2-3 (Dry CST)
Moisture Content from Analyzer (105°C)	--	5.48%	39.3%	40.0%	17.1%	9.24%
TGA Moisture Content at 105°C	5.23%	3.10%	32.5%	34.3%	19.0%	6.84%
TGA Moisture Content at 200°C	10.1%	8.60%	38.2%	38.6%	23.3%	11.3%
TGA Moisture Content at 400°C	16.3%	15.7%	42.2%	42.0%	28.5%	17.4%
TGA Change in Moisture (105 to 400°C)	11.1%	12.6%	9.7%	7.8%	9.6%	10.6%
SRNL = Savannah River National Laboratory						

---

[1] Moisture analysis of the Test 2 pre-test samples was inadvertently conducted at 160°C rather than 105°C. The impact on flammable gas rates is that G-values would be larger (conservative) than the values calculated using 105°C moisture analysis values.

Figure 6.1 shows a comparison of the as-received CST that was used in Test 2 compared to the data published by SRNL (Figure 3.4 in King et al. 2018b). The TGA traces are very similar to each other, which suggests that as-received CST material has similar moisture content if it has been protected from exposure to ambient air.[1] Figure 6.2 shows the TGA traces for the wet CST samples measured after testing, both rad and thermal systems, compared to the as-received CST. Figure 6.3 shows the TGA traces for the dry CST samples measured after testing, both rad and thermal systems, compared to the as-received CST.
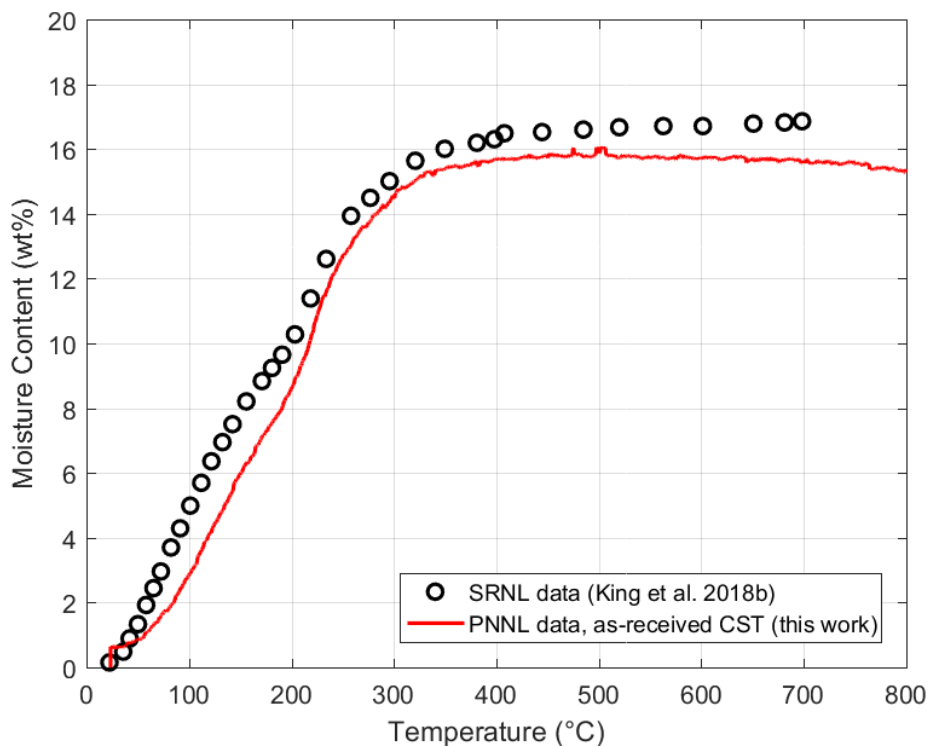
Figure 6.1. Comparison of the TGA results (FIO) for the CST used in this work for Test 2, and previously published results from SRNL.

---

[1] Although the CST measured by SRNL as reported by King et al. (2018b) had been onsite since 2001, it had remained in drums that were sealed. Thus, the CST was protected from moisture exposure over that time period. It is notable that the CST likely experienced thermal cycling because it spent some years of storage in a facility that was not climate-controlled. The SRNL CST and the PNNL CST were not of the same production lot and were produced many years apart.
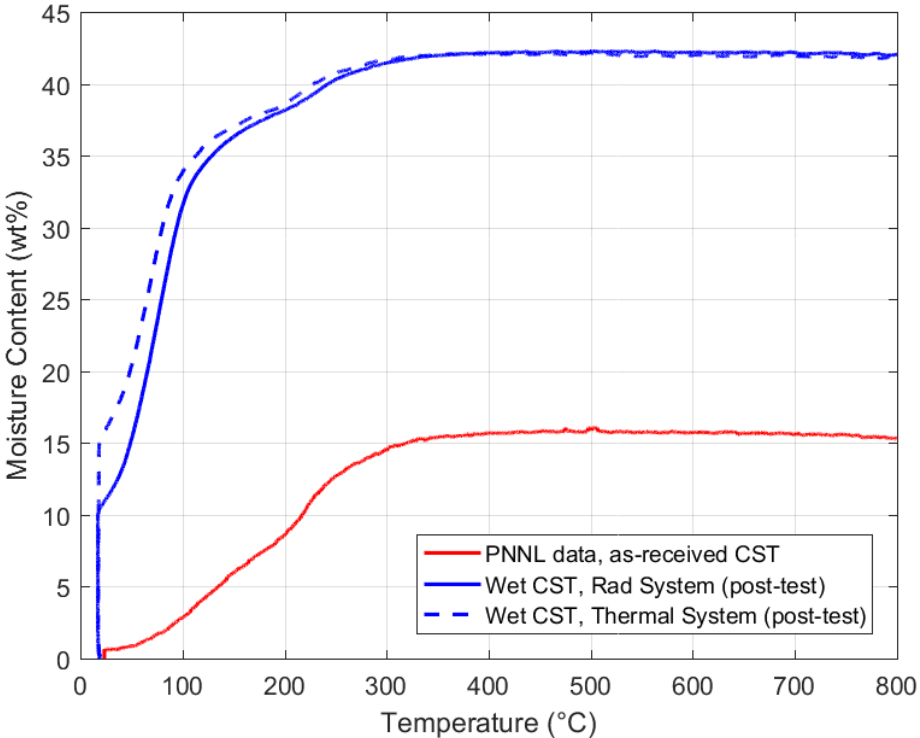
Figure 6.2. TGA results from wet CST post-testing (FIO).
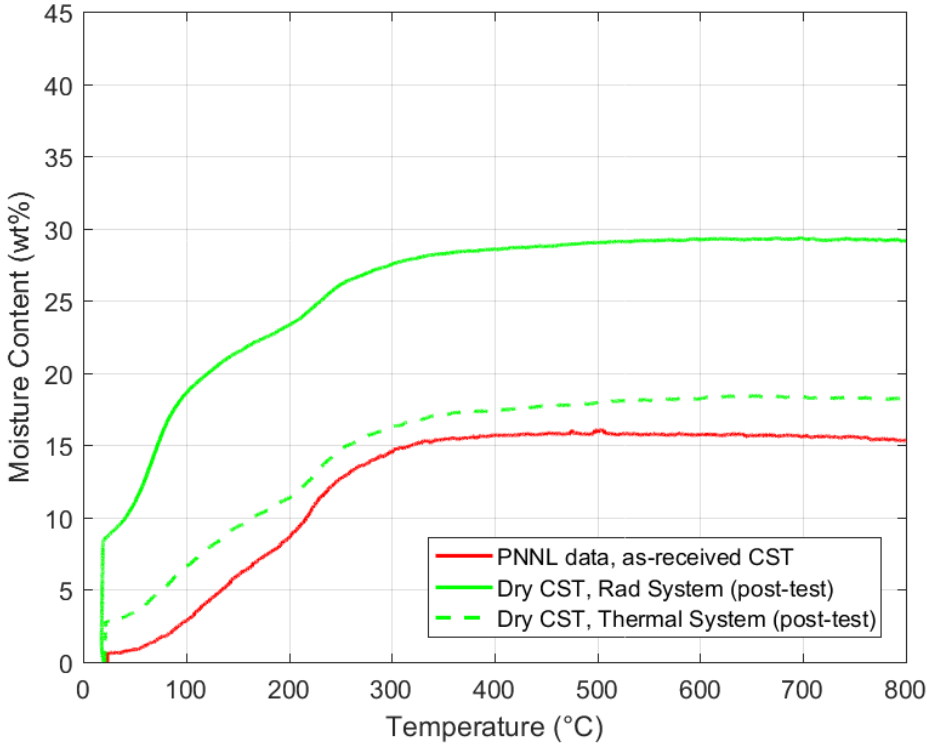
Figure 6.3. TGA results from dry CST post-test (FIO).

7.0 Conclusions

The gas generation of CST was tested in water, simulant, simulant with added organic carbon, free-drained wet CST, and free-drained dry CST. All conditions were tested at 25°C, and the simulant with added organic carbon was also tested at 70°C. All conditions were tested to total accumulated gamma dose of nominally 300 Mrad. The wet and dry CST were also tested to a total accumulated gamma dose of nominally 900 Mrad. The testing was conducted in two tests, and each test was conducted using a different lot of CST.[1] Overall, the greatest gas generation rate observed was the hydrogen generation of the CST in water. The $G(H_2)$-value of the CST in water was similar to that observed for water in contact with other ion exchange media (Colburn et al. 2018). The dry CST in Test 1 demonstrated the next-largest hydrogen generation, followed by the wet CST. This result was unforeseen because it was expected that radiolysis of the water would dominate the production of gas, and that the presence of higher amounts of water would generate more hydrogen gas. Both of these cases also had gradually increasing $G(H_2)$-values at each subsequent sampling event. To confirm that this behavior did not persist over longer durations, Test 2 conditions were adjusted to include an extended irradiation of the wet CST and dry CST to better understand the long-time trend in gas generation under potential storage conditions.

A key point to recall regarding the data is that although the $G(H_2)$-values for the wet and dry CST conditions were larger than anticipated and are on the order of the $G(H_2)$-value for CST in water, the cumulative number of moles generated per volume of CST bed for CST in water remained markedly higher, at least during the 300 Mrad period for which data were collected for all conditions. Thus, that result is expected to bound all scenarios for which there is less moisture (than full saturation) present in a column of CST. The $G(H_2)$-values are generated by normalizing to the mass of liquid that is present in the sample vessel; thus, higher $G(H_2)$-values when the CST is drier may indicate that the gas generation mechanism depends on more than just the presence of a specific amount of water and likely contains additional complexity.

When the $G(H_2)$-values were compared, the two CST lots had marked differences in gas generation, particularly in the wet CST condition. The gas generation of wet CST from the second lot of material (used in Test 2) was approximately 10% of what was observed in the first test (which used a different lot of CST). Although there was a small difference in the moisture content of the two wet CST samples tested, the difference was not great enough to explain the difference between the observed gas generation. The dry CST condition also was different by approximately a factor of 3 between the two lots; in this case, some of the difference may have been caused by the factor of 2 difference in the starting moisture content of the samples. The data indicate that there may be lot-to-lot variability that drives different gas generation behavior in similar test conditions; if the variability is a concern, then it would be prudent to examine the gas generation of additional lots of CST material to better understand the magnitude and mechanisms of the variation, particularly under storage conditions.

---

[1] Test 1 used the only lot of CST that was available at the time, of which there was a limited amount. Prior to Test 2, a new lot of CST was received that was used in a suite of testing at PNNL and is anticipated to be similar to the CST that will be used in DFLAW processing. For consistency with other CST test results, Test 2 used this new lot of CST as directed by WRPS.

8.0 References

Anderson KA. 2018. *Preliminary Early Direct-Feed Low-Activity Waste Flowsheet*. RPP-RPT-60521, Rev. 0, Washington River Protection Solutions, Richland, Washington.

Ard KE. 2019. *Specification for the Tank-Side Cesium Removal Demonstration Project (Project TD101)*. RPP-SPEC-61910, Rev. 1, Washington River Protection Solutions, Richland, Washington.

Bibler NE, CL Crawford, and CR Biddle. 1998. *Results of Scoping Studies for Determining Radiolytic Hydrogen Production from Moist CST and CST Slurries*. WSRC-RP-98-01143, Westinghouse Savannah River Company, Aiken, South Carolina.

Braun J and T Barker. 2012. "Fukushima Daiichi Emergency Water Treatment." *Nuclear Plant Journal* Jan-Feb 2012:36-37.

Bryan SA and LR Pederson. 1994. *Composition, Preparation, and Gas Generation Results from Simulated Wastes of Tank 241-SY-101*. PNL-10075, Pacific Northwest Laboratory, Richland, Washington.

Bryan SA and LR Pederson. 1995. *Thermal and Combined Thermal and Radiolytic Reactions Involving Nitrous Oxide, Hydrogen, and Nitrogen in the Gas Phase; Comparison of Gas Generation Rates in Supernate and Solid Fractions of Tank 241-SY-101 Simulated Waste*. PNL-10490, Pacific Northwest Laboratory, Richland, Washington.

Bryan SA, CM King, LR Pederson, SV Forbes, and RL Sell. 1996. *Gas Generation from Tank 241-SY-103 Waste*. PNNL-10978, Pacific Northwest National Laboratory, Richland, Washington.

Chew DP, BA Hamm, and MN Wells. 2019. *Liquid Waste System Plan Revision 21*. SRR-LWP-2009-00001, Revision 21, Savannah River Remediation, Aiken, South Carolina.

Colburn HA, SA Bryan, DM Camaioni, LA Mahoney, and SR Adami. 2018. *Gas Generation Testing of Spherical Resorcinol-Formaldehyde (sRF) Resin*. PNNL-26869, Rev. 0 (RPT-LPIST-002, Rev. 0), Pacific Northwest National Laboratory, Richland, Washington.

Fiskum SK, HA Colburn, RA Peterson, AM Rovira, and MR Smoot. 2018. *Cesium Ion Exchange Using Crystalline Silicotitanate with 5.6 M Sodium Simulant*. PNNL-27587, Pacific Northwest National Laboratory, Richland, Washington.

Fiskum SK, AM Rovira, JR Allred, HA Colburn, MR Smoot, AM Carney, TT Trang-Le, MG Cantaloub, EC Buck, and RA Peterson. 2019. *Cesium Removal from Tank Waste Simulants Using Crystalline Silicotitanate at 12% and 100% TSCR Bed Heights*. PNNL-28527, Rev. 0 (RPT-DFTP-008, Rev. 0), Pacific Northwest National Laboratory, Richland, Washington.

Gauglitz PA, CLH Bottenus, GK Boeringa, CA Burns, and PP Schonewill. 2019. *Drying of Crystalline Silicotitanate (CST) Beds by Air Flow*. PNNL-28673, Rev. 0 (RPT-LPTTS-003, Rev.0). Pacific Northwest National Laboratory, Richland, Washington.

Hamm LL, T Hang, DJ McCabe, and WD King. 2002. *Preliminary Ion Exchange Modeling for Removal of Cesium from Hanford Waste Using Hydrous Crystalline Silicotitanate Material*. WSRC-TR-2001-00400, Westinghouse Savannah River Company, Aiken, South Carolina.

King CM, LR Pederson, and SA Bryan. 1997. *Thermal and Radiolytic Gas Generation from Tank 241-S-102 Waste*. PNNL-11600, Pacific Northwest National Laboratory, Richland, Washington.

King CM and SA Bryan. 1999. *Thermal and Radiolytic Gas Generation Tests on Material from Tanks 241-U-103, 241-AW-101, 241-S-106, and 241-S-102: Status Report*. PNNL-12181, Pacific Northwest National Laboratory, Richland, Washington.

King WD, LL Hamm, CJ Coleman, FF Fondeur, and SH Reboul. 2018a. Crystalline Silicotitanate (CST) Ion Exchange Media Performance Evaluations in SRS Average Supernate Simulant and Tank 10H Waste Solution to Support TCCR. SRNL-STI-2018-00277, Rev. 0, Savannah River National Laboratory, Aiken, South Carolina.

King WD, LL Hamm, DJ McCabe, CA Nash, and FF Fondeur. 2018b. *Crystalline Silicotitanate Ion Exchange Media Long-Term Storage Evaluation*. SRNL-STI-2018-00567, Rev. 0, Savannah River National Laboratory, Aiken, South Carolina.

Mahoney LA. 2015. *Self-Flammability of Gases Generated by Hanford Tank Waste and the Potential of Nitrogen Inerting to Eliminate Flammability Safety Concerns*. PNNL-24194, Rev. 1 (WTP-RPT-237, Rev. 1), Pacific Northwest National Laboratory, Richland, Washington.

McCabe DJ. 1997. Examination of Crystalline Silicotitanate and Applicability in Removal of Cesium from SRS High Level Waste. WSRC-TR-97-0016, Westinghouse Savannah River Company, Aiken, SC.

McCabe DJ. 2004. *Calculation of the Hydrogen Gas Generation in Small Cesium-Removal Columns Containing Crystalline Silicotitanate*. WSRC-RP-2004-00164, Rev. 0, Westinghouse Savannah River Company, Aiken, SC.

Pease LF, SK Fiskum, HA Colburn, and PP Schonewill. 2019. *Cesium Ion Exchange with Crystalline Silicotitanate: Literature Review*. PNNL-28343, Rev. 0 (RPT-LPTTS-001, Rev. 0), Pacific Northwest National Laboratory, Richland, Washington.

Rovira AM, SK Fiskum, HA Colburn, JR Allred, MR Smoot, and RA Peterson. 2018. *Cesium Ion Exchange Testing Using Crystalline Silicotitanate with Hanford Tank Waste 241-AP-107*. PNNL-27706 (RPT-DFTP-011, Rev. 0). Pacific Northwest National Laboratory, Richland, Washington.

Rovira AM, SK Fiskum, HA Colburn, JR Allred, MR Smoot, RA Peterson and KA Colosi. 2019a. "Cesium Ion Exchange Testing Using Crystalline Silicotitanate with Hanford Tank Waste 241-AP-107." *Separation Science and Technology* 54(12): 1942-1951. doi:10.1080/01496395.2019.1577273

Rovira AM, SK Fiskum, JR Allred, JGH Geeting, HA Colburn, AM Carney, and TT Trang-Le. 2019b. *Dead-End Filtration and Crystalline Silicotitanate Cesium Ion Exchange with Hanford Tank Waste AW-102*. PNNL-28783, Rev. 0 (RPT-TCT-003, Rev. 0). Pacific Northwest National Laboratory, Richland, Washington.

Russell RL, PP Schonewill, and CA Burns. 2017. *Simulant Development for LAWPS Testing*. PNNL-26165, Rev. 0 (RPT-LPIST-001, Rev. 0), Pacific Northwest National Laboratory, Richland, Washington.

Swyler KJ and RE Barletta. 1983. Irradiation of zeolite ion-exchange media: Electron beams and gamma rays; IE-95 is decontamination medium at Three Mile Island Unit II. NUREG/CR-2785, Brookhaven National Laboratory, Upton, New York.

Tilanus SN, LM Bergmann, RO Lokken, AJ Schubick, EB West, RT Jasper, SL Orcutt, TM Holh, AN Praga, MN Wells, KW Burnett, CS Smalley, JK Bernards, SD Reaksecker, and TL Waldo. 2017. *River Protection Project System Plan*, ORP-11242, Revision 8. DOE Office of River Protection, Richland, Washington.

Walker Jr. JF, PA Taylor, RL Cummins, BS Evans, SD Heath, JD Hewitt, RD Hunt, HL Jennings, JA Kilby, DD Lee, S Lewis-Lambert, SA Richardson, and RF Utrera. 1998. *Cesium Removal Demonstration Utilizing Crystalline Silicotitanate Sorbent for Processing Melton Valley Storage Tank Supernatant: Final Report*. ORNL/TM-13503. Oak Ridge National Laboratory, Oak Ridge, Tennessee.

Walker DD, DJ Adamson, TD Allen, RW Blessing, WT Boyce, BH Croy, RA Dewberry, DP Diprete, SD Fink, T Hang, JC Hart, MC Lee, JJ Olson, and MJ Whitaker. 1999. *Cesium Removal from Savannah River Site Radioactive Waste Using Crystalline Silicotitanate (IONSIV IE-911)*. WSRC-TR-99-00308, Westinghouse Savannah River Company, Aiken, South Carolina.

Walker DD. 2003. *Radiolytic Gas Generation in Crystalline Silicotitanate Slurries*. WSRC-TR-99-00285, Rev. 1, Westinghouse Savannah River Company, Aiken, South Carolina.

Appendix A – Gas Composition Analysis Results

The data in this appendix is the composition of gas observed in each sample collected for Test 1 and Test 2. Replicate test conditions are tabulated together for each sample set; refer to Table 4.4 and Table 4.5 (Test 1) and Table 4.6 and Table 4.7 (Test 2) for a crosswalk between the vessel number and the corresponding experimental conditions. Tables A.1 through A.8 contain the compositional data from Test 1, and Tables A.9 through A.16 contain the same from Test 2.

Note that the headings "Other HC" represents "Other Hydrocarbons" and "Other N" represents "Other Nitrogen" compounds measured in the composition analysis. Other, in this case, means any hydrocarbon or nitrogen gases besides those already quantified in each table.

Table A.1. Percent Composition of Gas in Samples – Water+CST data, 25°C, Rad System.

Sample	Laboratory ID	Δ Time (hr)	Cumulative Run Time (hr)	Δ Dose (Mrad)	Mole Percent Gas, 25 °C												
					H_2	He-3	He	CH_4	N_2	O_2	Ne	C_2H_6	CO	Ar	CO_2	Other HC	Other N
	G-2-130-1	162.50	162.50	95.6	19.5	0.036	0.029	0.074	1.55	0.308	<0.001	0.211	<0.001	78.10	<0.001	0.100	0.063
Test 1, Vessel 1-1	G-2-136-1	172.58	335.08	101	27.1	<0.001	<0.001	0.061	0.124	5.5	<0.001	0.154	<0.001	67.1	<0.001	<0.001	0.042
	G-2-144-1	214.25	549.33	126	30.5	0.066	<0.001	0.041	0.117	11.5	<0.001	0.110	<0.001	57.7	<0.001	<0.001	0.032
	G-2-130-5	162.50	162.50	95.6	27.7	<0.001	<0.001	0.17	0.857	0.482	<0.001	0.038	<0.001	70.9	<0.001	<0.001	0.066
Test 1, Vessel 1-5	G-2-136-5	172.58	335.08	101	28.4	0.061	<0.001	0.017	0.362	6.5	1.75	0.049	<0.001	62.9	<0.001	<0.001	0.013
	G-2-144-5	214.25	549.33	126	35.6	<0.001	<0.001	<0.001	0.082	13.2	<0.001	0.049	<0.001	51.1	<0.001	0.039	0.012

Table A.2. Percent Composition of Gas in Samples – Wet CST, 25°C, Rad System.

Sample	Laboratory ID	Δ Time (hr)	Cumulative Run Time (hr)	Δ Dose (Mrad)	Mole Percent Gas, 25 °C												
					H_2	He-3	He	CH_4	N_2	O_2	Ne	C_2H_6	CO	Ar	CO_2	Other HC	Other N
	G-2-130-2	162.50	162.50	95.6	9.63	<0.001	0.029	0.076	1.380	0.0870	1.12	0.14	<0.001	87.50	<0.001	<0.001	0.028
Test 1, Vessel 1-2	G-2-136-2	172.58	335.08	101	12.9	<0.001	<0.001	0.025	0.41	1.12	<0.001	0.082	<0.001	85.5	<0.001	<0.001	0.011
	G-2-144-2	214.25	549.33	126	16.7	<0.001	<0.001	<0.001	0.272	4.50	<0.001	0.050	<0.001	78.5	<0.001	<0.001	<0.001
	G-2-130-6	162.50	162.50	95.6	7.89	0.018	<0.001	0.013	0.626	0.070	<0.001	<0.001	<0.001	91.4	not reported	<0.001	<0.001
Test 1, Vessel 1-6	G-2-136-6	172.58	335.08	101	12.8	<0.001	<0.001	<0.001	1.31	1.87	<0.001	<0.001	<0.001	84.0	0.001	<0.001	<0.001
	G-2-144-6	214.25	549.33	126	17.0	0.061	<0.001	<0.001	0.292	5.2	<0.001	<0.001	<0.001	77.4	<0.001	0.083	<0.001

Table A.3. Percent Composition of Gas in Samples – Dry CST, 25°C, Rad System.

Sample	Laboratory ID	Δ Time (hr)	Cumulative Run Time (hr)	Δ Dose (Mrad)	Mole Percent Gas, 25 °C												
					H_2	He-3	He	CH_4	N_2	O_2	Ne	C_2H_6	CO	Ar	CO_2	Other HC	Other N
Test 1, Vessel 1-3	G-2-130-3	162.50	162.50	95.6	14.70	<0.001	0.035	0.061	1.14	0.54	<0.001	0.141	<0.001	83.35	<0.001	<0.001	0.060
	G-2-136-3	172.58	335.08	101	16.1	0.048	<0.001	0.024	1.11	3.5	<0.001	0.081	<0.001	79.1	<0.001	<0.001	0.024
	G-2-144-3	214.25	549.33	126	19.9	<0.001	<0.001	<0.001	0.46	6.7	<0.001	0.064	<0.001	72.9	<0.001	<0.001	0.017
Test 1, Vessel 1-7	G-2-130-7	162.50	162.50	95.6	12.2	<0.001	<0.001	<0.001	0.556	0.488	<0.001	<0.001	<0.001	86.8	<0.001	<0.001	0.2
	G-2-136-7	172.58	335.08	101	15.8	<0.001	<0.001	<0.001	1.04	3.99	<0.001	<0.001	<0.001	79.1	<0.001	<0.001	<0.001
	G-2-144-7	214.25	549.33	126	17.4	0.083	0.037	<0.001	0.39	6.0	<0.001	<0.001	<0.001	76.1	<0.001	<0.001	0.021

Table A.4. Percent Composition of Gas in Samples – CST in 5.6M Na Simulant, 25°C, Rad System.

Sample	Laboratory ID	Δ Time (hr)	Cumulative Run Time (hr)	Δ Dose (Mrad)	Mole Percent Gas, 25 °C												
					H_2	He-3	He	CH_4	N_2	O_2	Ne	C_2H_6	CO	Ar	CO_2	Other HC	Other N
Test 1, Vessel 1-4	G-2-130-4	162.50	162.50	95.6	5.40	<0.001	<0.001	<0.001	0.460	6.41	<0.001	0.019	<0.001	87.5	<0.001	0.085	0.093
	G-2-136-4	172.58	335.08	101	7.6	<0.001	0.016	0.018	0.35	10.8	1.28	<0.001	<0.001	79.8	<0.001	0.060	0.126
	G-2-144-4	214.25	549.33	126	9.1	<0.001	<0.001	0.018	0.110	13.3	<0.001	0.021	<0.001	77.3	<0.001	0.050	0.127
Test 1, Vessel 1-8	G-2-130-8	162.50	162.50	95.6	8.07	<0.001	<0.001	<0.001	4.17	19.3	<0.001	0.029	<0.001	68.3	<0.001	0.075	0.067
	G-2-136-8	172.58	335.08	101	8.9	<0.001	0.052	<0.001	0.38	23.6	<0.001	0.034	<0.001	67.0	<0.001	<0.001	0.089
	G-2-136-8-Run#2	172.58	335.08	101	8.9	0.045	0.040	<0.001	0.38	23.6	<0.001	<0.001	<0.001	67.0	<0.001	<0.001	0.057
	G-2-144-8	214.25	549.33	126	10.9	<0.001	<0.001	<0.001	0.088	26.0	<0.001	<0.001	<0.001	62.9	<0.001	<0.001	0.068
	G-2-144-8-Run#2	214.25	549.33	126	10.8	<0.001	<0.001	<0.001	0.088	25.7	1.33	<0.001	<0.001	62.1	<0.001	<0.001	0.063

Table A.5. Percent Composition of Gas in Samples – CST in water, 25°C, Thermal System.

Sample	Laboratory ID	Δ Time (hr)	Cumulative Run Time (hr)	Mole Percent Gas, 25 °C												
				H_2	He-3	He	CH_4	N_2	O_2	Ne	C_2H_6	CO	Ar	CO_2	Other HC	Other N
Test 1, Vessel 2-1	G-2-131-1	161.08	162.50	<0.001	<0.001	<0.001	0.037	0.219	0.056	<0.001	0.112	<0.001	99.54	<0.001	<0.001	0.035
	G-2-137-1-Run-2	172.58	335.08	<0.001	0.062	0.017	0.031	0.214	0.052	1.83	0.071	<0.001	97.62	<0.001	0.077	0.03
	G-2-137-1-Run#3	214.25	549.33	<0.001	<0.001	<0.001	0.010	0.209	0.040	0.99	0.070	<0.001	98.65	<0.001	<0.001	0.033
	G-2-145-1	214.25	549.33	0.030	<0.001	0.097	0.020	0.174	<0.001	<0.001	0.012	<0.001	99.58	<0.001	<0.001	0.052
Test 1, Vessel 2-5	G-2-131-5	162.50	162.50	<0.001	<0.001	<0.001	<0.001	0.395	0.135	<0.001	<0.001	<0.001	99.470	<0.001	<0.001	<0.001
	G-2-137-5	172.58	335.08	<0.001	<0.001	<0.001	<0.001	0.251	0.022	<0.001	<0.001	<0.001	99.73	<0.001	<0.001	<0.001
	G-2-145-5	214.25	549.33	<0.001	<0.001	0.041	<0.001	0.324	0.066	<0.001	<0.001	<0.001	99.54	<0.001	<0.001	0.022

Table A.6. Percent Composition of Gas in Samples – Wet CST, 25°C, Thermal System.

Sample	Laboratory ID	Δ Time (hr)	Cumulative Run Time (hr)	Mole Percent Gas, 25 °C												
				H_2	He-3	He	CH_4	N_2	O_2	Ne	C_2H_6	CO	Ar	CO_2	Other HC	Other N
Test 1, Vessel 2-2	G-2-131-2	162.50	162.50	0.015	<0.001	0.03	<0.001	0.228	0.097	0.950	0.032	<0.001	98.54	<0.001	0.101	0.009
	G-2-137-2	172.58	335.08	0.010	0.058	<0.001	<0.001	0.216	0.066	<0.001	<0.001	<0.001	99.55	<0.001	0.085	0.019
	G-2-145-2	214.25	549.33	0.023	<0.001	<0.001	<0.001	0.345	0.067	1.21	<0.001	<0.001	98.35	<0.001	<0.001	<0.001
Test 1, Vessel 2-6	G-2-131-6	162.50	162.50	0.025	<0.001	0.037	0.274	12.7	3.38	<0.001	0.805	<0.001	82.8	<0.001	<0.001	0.046
	G-2-137-6	172.58	331.00	0.018	<0.001	<0.001	0.029	0.704	0.032	<0.001	0.074	<0.001	99.53	<0.001	0.080	0.038
	G-2-145-6	214.00	545.00	0.010	<0.001	<0.001	0.017	0.126	0.019	<0.001	0.051	<0.001	99.75	<0.001	<0.001	0.030

Table A.7. Percent Composition of Gas in Samples – Dry CST, 25°C, Thermal System.

| Sample | Laboratory ID | Δ Time (hr) | Cumulative Run Time (hr) | Mole Percent Gas, 25 °C | | | | | | | | | | | | |
				H_2	He-3	He	CH_4	N_2	O_2	Ne	C_2H_6	CO	Ar	CO_2	Other HC	Other N
Test 1, Vessel 2-3	G-2-131-3	161.08	161.08	0.014	<0.001	<0.001	<0.001	0.331	0.103	0.881	0.051	<0.001	98.56	<0.001	<0.001	0.058
	G-2-131-3-DUP	161.08	331.00	0.012	<0.001	<0.001	<0.001	0.331	0.104	0.746	<0.001	<0.001	98.65	<0.001	0.093	0.054
	G-2-137-3	169.92	331.00	0.021	<0.001	<0.001	<0.001	0.120	0.022	0.95	0.023	<0.001	98.80	<0.001	0.044	0.028
	G-2-145-3	214.00	545.00	<0.001	<0.001	<0.001	<0.001	0.099	0.014	<0.001	<0.001	<0.001	99.82	<0.001	0.066	<0.001
Test 1, Vessel 2-7	G-2-131-7	161.08	161.08	<0.001	<0.001	<0.001	0.151	0.86	0.215	<0.001	0.52	<0.001	98.00	<0.001	0.147	0.121
	G-2-137-7	169.92	331.00	0.005	<0.001	<0.001	0.055	0.202	0.057	<0.001	0.193	<0.001	99.33	<0.001	0.088	0.073
	G-2-145-7	214.00	545.00	0.017	<0.001	<0.001	0.045	0.116	0.017	<0.001	0.172	<0.001	99.56	0.014	0.076	<0.001

Table A.8. Percent Composition of Gas in Samples – CST in 5.6M Na Simulant, 25°C, Thermal System.

| Sample | Laboratory ID | Δ Time (hr) | Cumulative Run Time (hr) | Mole Percent Gas, 25 °C | | | | | | | | | | | | |
				H_2	He-3	He	CH_4	N_2	O_2	Ne	C_2H_6	CO	Ar	CO_2	Other HC	Other N
Test 1, Vessel 2-4	G-2-131-4	161.08	161.08	0.013	<0.001	<0.001	0.005	14.8	3.93	<0.001	0.004	<0.001	81.1	<0.001	<0.001	0.028
	G-2-137-4	169.92	331.00	0.022	<0.001	<0.001	<0.001	0.082	0.010	<0.001	<0.001	<0.001	99.81	<0.001	0.073	<0.001
	G-2-145-4	214.00	545.00	0.019	<0.001	0.032	<0.001	0.104	0.036	<0.001	0.016	<0.001	99.71	<0.001	0.082	<0.001
Test 1, Vessel 2-8	G-2-131-8	161.08	161.08	0.001	<0.001	0.045	0.068	1.720	0.426	<0.001	0.211	<0.001	97.4	<0.001	0.129	0.0387
	G-2-137-8	169.92	331.00	<0.001	<0.001	0.016	0.020	22.7	5.9	<0.001	0.060	<0.001	71.2	<0.001	0.056	0.031
	G-2-145-8	214.00	545.00	<0.001	<0.001	<0.001	<0.001	0.171	0.074	1.76	0.036	<0.001	97.92	<0.001	<0.001	0.011
	G-2-145-8-Run#2	214.00	545.00	<0.001	<0.001	<0.001	<0.001	0.177	0.0670	1.71	0.025	<0.001	98.01	<0.001	<0.001	0.013

Table A.9. Percent Composition of Gas in Samples – Wet CST, 25°C, Rad System.

Sample	Laboratory ID	Δ Time (hr)	Cumulative Run Time (hr)	Δ Dose (Mrad)	Mole Percent Gas, 25 °C											
					H_2	He-3	He	CH_4	N_2	O_2	Ne	C_2H_6	CO	Ar	CO_2 /N_2O	Other HC
Test 2, Vessel 1-1	G-2-157-1	126.75	126.75	70.6	1.28	<0.001	<0.001	<0.001	0.94	0.116	<0.001	0.007	<0.001	97.63	0.022	<0.001
	G-3-2-1	208.92	335.67	116	2.09	<0.001	<0.001	<0.001	0.31	0.042	<0.001	0.004	<0.001	97.54	0.02	<0.001
	G-3-11-1	192.42	528.08	107	1.965	0.02	0.004	0.008	9.205	2.610	<0.001	0.010	<0.001	86.14	0.04	0.006
	G-3-16-1	167.75	695.83	93.4	1.870	<0.001	<0.001	<0.001	0.229	0.351	<0.001	0.010	<0.001	97.52	0.03	<0.001
	G-3-20-1	194.42	890.25	108	2.36	<0.001	<0.001	<0.001	0.284	0.51	<0.001	<0.001	<0.001	96.81	0.03	<0.001
	G-3-25-1	145.92	1036.17	81.3	2.14	<0.001	<0.001	0.004	0.184	0.59	<0.001	0.005	<0.001	97.05	0.02	<0.001
	G-3-30-1	166.33	1202.50	92.6	2.28	<0.001	<0.001	<0.001	0.173	0.59	<0.001	<0.001	<0.001	96.93	0.03	<0.001
	G-3-36-1	164.42	1366.92	91.6	2.25	<0.001	<0.001	<0.001	0.139	0.66	<0.001	<0.001	<0.001	96.93	0.02	<0.001
	G-3-44-1	263.42	1630.33	147	3.81	<0.001	<0.001	<0.001	0.186	1.12	<0.001	0.005	<0.001	94.84	0.03	<0.001
Test 2, Vessel 1-5	G-2-157-5	126.75	126.75	70.6	1.71	<0.001	<0.001	<0.001	0.52	0.075	<0.001	0.005	<0.001	97.7	0.03	<0.001
	G-3-2-5	208.92	335.67	116	2.95	<0.001	<0.001	<0.001	1.43	0.49	<0.001	<0.001	<0.001	95.10	0.03	<0.001
	G-3-11-5	192.42	528.08	107	2.97	<0.001	<0.001	0.006	5.6	2.11	<0.001	<0.001	<0.001	89.2	0.03	<0.001
	G-3-16-5	167.75	695.83	93.4	2.9	<0.001	<0.001	<0.001	0.179	0.87	<0.001	<0.001	<0.001	95.97	0.03	<0.001
	G-3-20-5	194.42	890.25	108	3.46	<0.001	<0.001	<0.001	0.166	1.06	<0.001	<0.001	<0.001	95.27	0.04	<0.001
	G-3-25-5	145.92	1036.17	81.3	2.66	<0.001	<0.001	<0.001	0.159	0.86	<0.001	<0.001	<0.001	96.30	0.03	<0.001
	G-3-30-5	166.33	1202.50	92.6	3.08	<0.001	<0.001	0.005	0.142	1.03	<0.001	<0.001	<0.001	95.71	0.02	<0.001
	G-3-36-5	164.42	1366.92	91.6	3.18	<0.001	<0.001	<0.001	0.133	1.11	<0.001	<0.001	<0.001	95.55	0.02	<0.001
	G-3-44-5	263.42	1630.33	147	5.6	<0.001	<0.001	<0.001	0.174	1.88	<0.001	<0.001	<0.001	92.3	0.03	<0.001

Table A.10. Percent Composition of Gas in Samples – Dry CST, 25°C, Rad System

| Sample | Laboratory ID | Δ Time (hr) | Cumulative Run Time (hr) | Δ Dose (Mrad) | Mole Percent Gas, 25 °C | | | | | | | | | | | |
					H_2	He-3	He	CH_4	N_2	O_2	Ne	C_2H_6	CO	Ar	CO_2 /N_2O	Other HC
	G-2-157-3	126.75	126.75	70.6	1.70	0.021	<0.001	<0.001	2.39	0.06	<0.001	<0.001	<0.001	95.8	0.05	<0.001
	G-3-2-3	208.92	335.67	116	3.0	<0.001	<0.001	<0.001	0.839	0.029	<0.001	<0.001	<0.001	96.1	0.03	0.002
	G-3-11-3	192.42	528.08	107	2.50	<0.001	<0.001	0.011	0.287	0.026	<0.001	0.006	<0.001	97.15	0.02	<0.001
	G-3-16-3	167.75	695.83	93.4	2.24	<0.001	<0.001	0.009	0.174	0.026	<0.001	<0.001	<0.001	97.52	0.02	<0.001
Test 2, Vessel 1-3	G-3-20-3	194.42	890.25	108	2.42	<0.001	<0.001	0.010	0.141	0.025	<0.001	<0.001	<0.001	97.39	0.02	<0.001
	G-3-25-3	145.92	1036.17	81.3	1.89	<0.001	<0.001	0.007	0.157	0.028	<0.001	<0.001	<0.001	97.89	0.03	<0.001
	G-3-30-3	166.33	1202.50	92.6	1.86	<0.001	<0.001	<0.001	0.155	0.024	<0.001	<0.001	<0.001	97.94	0.02	<0.001
	G-3-36-3	164.42	1366.92	91.6	1.83	<0.001	<0.001	0.006	0.170	0.022	<0.001	<0.001	<0.001	97.95	0.02	<0.001
	G-3-44-3	263.42	1630.33	147	2.37	<0.001	<0.001	0.007	0.249	0.029	<0.001	<0.001	<0.001	97.31	0.03	<0.001
	G-2-157-7	126.75	126.75	70.6	1.73	<0.001	0.013	<0.001	2.26	0.084	<0.001	<0.001	<0.001	95.9	0.03	<0.001
	G-3-2-7	208.92	335.67	116	2.94	<0.001	<0.001	<0.001	3.55	0.80	<0.001	<0.001	<0.001	92.7	0.03	<0.001
	G-3-11-7	192.42	528.08	107	2.51	<0.001	<0.001	0.008	0.25	0.023	<0.001	<0.001	<0.001	97.2	0.02	<0.001
	G-3-16-7	167.75	695.83	93.4	2.25	0.015	<0.001	0.010	0.154	0.024	<0.001	<0.001	<0.001	97.52	0.03	0.003
Test 2, Vessel 1-7	G-3-20-7	194.42	890.25	108	2.02	0.032	<0.001	0.022	1.61	0.443	<0.001	0.016	<0.001	95.81	0.05	<0.001
	G-3-25-7	145.92	1036.17	81.3	1.93	<0.001	<0.001	0.010	0.135	0.028	<0.001	0.00632	<0.001	97.87	0.02	<0.001
	G-3-30-7	166.33	1202.50	92.6	1.90	<0.001	0.026	0.014	0.144	0.028	<0.001	<0.001	<0.001	97.86	0.03	<0.001
	G-3-36-7	164.42	1366.92	91.6	1.95	<0.001	0.018	0.006	0.157	0.028	<0.001	<0.001	<0.001	97.81	0.03	<0.001
	G-3-44-7	263.42	1630.33	147	2.48	<0.001	0.01	0.007	0.223	0.032	<0.001	<0.001	<0.001	97.22	0.03	0.002

Table A.11. Percent Composition of Gas in Samples – Simulant w/ TOC + CST, 25°C, Rad System

Sample	Laboratory ID	Δ Time (hr)	Cumulative Run Time (hr)	Δ Dose (Mrad)	Mole Percent Gas, 25 °C											
					H_2	He-3	He	CH_4	N_2	O_2	Ne	C_2H_6	CO	Ar	N_2O	Other HC
Test 2, Vessel 1-2	G-2-157-2	126.75	126.75	71.1	4.13	<0.001	<0.001	<0.001	11.3	0.262	<0.001	0.009	<0.001	55.1	29.1	0.003
	G-2-162-2	88.83	215.58	49.8	5.0	0.020	<0.001	<0.001	9.7	0.091	<0.001	0.015	<0.001	70.0	15.3	0.002
	G-3-2-2	120.08	335.67	67.4	7.2	<0.001	<0.001	<0.001	9.5	0.235	<0.001	0.024	<0.001	74.8	8.2	<0.001
	G-3-11-2	192.42	528.08	108	11.9	<0.001	<0.001	0.013	8.2	2.82	<0.001	0.020	<0.001	70.5	6.7	0.003
Test 2, Vessel 1-6	G-2-157-6	126.75	126.75	71.1	7.0	<0.001	<0.001	<0.001	10.8	0.167	<0.001	0.009	<0.001	60.1	21.9	0.002
	G-2-162-6	88.83	215.58	49.8	5.9	<0.001	<0.001	<0.001	8.3	0.152	<0.001	0.009	<0.001	78.10	7.5	<0.001
	G-3-2-6	120.08	335.67	67.4	8.7	<0.001	<0.001	<0.001	10.7	1.58	<0.001	0.015	<0.001	75.0	4.02	<0.001
	G-3-11-6	192.42	528.08	108	12.9	<0.001	<0.001	0.013	5.1	3.5	<0.001	0.014	<0.001	73.7	4.8	<0.001

Table A.12. Percent Composition of Gas in Samples – Simulant w/ TOC + CST, 70°C, Rad System

Sample	Laboratory ID	Δ Time (hr)	Cumulative Run Time (hr)	Δ Dose (Mrad)	Mole Percent Gas, 25 °C											
					H_2	He-3	He	CH_4	N_2	O_2	Ne	C_2H_6	CO	Ar	N_2O	Other HC
Test 2, Vessel 1-4	G-2-157-4	126.75	126.75	71.1	7.2	<0.001	<0.001	<0.001	12.55	0.175	<0.001	0.043	<0.001	51.2	28.9	0.009
	G-2-162-4	88.83	215.58	49.8	7.70	<0.001	<0.001	<0.001	9.1	0.064	<0.001	0.019	<0.001	72.9	10.2	0.004
	G-3-2-4	120.08	335.67	67.4	10.4	<0.001	<0.001	<0.001	11.1	2.29	<0.001	0.010	<0.001	71.9	4.3	<0.001
	G-3-11-4	192.42	528.08	108	15.4	<0.001	0.020	0.018	8.9	5.3	<0.001	<0.001	<0.001	62.6	7.8	0.002
Test 2, Vessel 1-8	G-2-157-8	126.75	126.75	71.1	7.9	<0.001	<0.001	<0.001	13.5	0.173	<0.001	0.033	<0.001	52.3	26.1	0.005
	G-2-162-8	88.83	215.58	49.8	8.37	0.01	<0.001	<0.001	9.353	0.063	<0.001	0.016	<0.001	74.71	7.475	<0.001
	G-3-2-8	120.08	335.67	67.4	12.2	0.008	<0.001	<0.001	10.5	1.40	<0.001	0.008	<0.001	72.6	3.24	<0.001
	G-3-11-8	192.42	528.08	108	16.2	0.018	<0.001	0.017	5.6	1.02	<0.001	<0.001	<0.001	67.9	9.3	0.002

Table A.13. Percent Composition of Gas in Samples – Wet CST, 25°C, Thermal System

| Sample | Laboratory ID | Δ Time (hr) | Cumulative Run Time (hr) | Mole Percent Gas, 25 °C | | | | | | | | | | | |
				H_2	He-3	He	CH_4	N_2	O_2	Ne	C_2H_6	CO	Ar	CO_2 /N_2O	Other HC
Test 2, Vessel 2-1	G-2-158-1	123.00	123.00	0.012	<0.001	<0.001	<0.001	1.80	1.00	<0.001	<0.001	<0.001	97.20	0.03	<0.001
	G-3-3-1	209.17	332.17	0.013	<0.001	<0.001	<0.001	0.80	0.336	<0.001	<0.001	<0.001	98.83	0.02	<0.001
	G-3-12-1	192.33	524.50	0.013	<0.001	<0.001	<0.001	0.260	0.096	<0.001	<0.001	<0.001	99.61	0.02	<0.001
	G-3-17-1	168.00	692.50	0.008	<0.001	<0.001	<0.001	0.136	0.052	<0.001	<0.001	<0.001	99.79	0.02	<0.001
	G-3-21-1	194.42	886.92	0.014	<0.001	<0.001	<0.001	0.140	0.052	<0.001	<0.001	<0.001	99.77	0.03	<0.001
	G-3-26-1	146.33	1033.25	0.015	<0.001	<0.001	<0.001	0.147	0.055	<0.001	<0.001	<0.001	99.76	0.02	<0.001
	G-3-31-1	165.83	1199.08	0.014	<0.001	<0.001	<0.001	0.176	0.072	<0.001	<0.001	<0.001	99.72	0.02	<0.001
	G-3-37-1	164.42	1363.50	0.009	<0.001	<0.001	<0.001	0.35	0.142	<0.001	<0.001	<0.001	99.48	0.02	<0.001
	G-3-45-1	263.42	1626.92	0.014	<0.001	<0.001	<0.001	0.18	0.056	<0.001	<0.001	<0.001	99.73	0.02	<0.001
Test 2, Vessel 2-5	G-2-158-5	123.00	123.00	0.018	<0.001	<0.001	<0.001	0.50	0.135	<0.001	<0.001	<0.001	99.31	0.03	0.004
	G-3-3-5	209.17	332.17	0.015	0.014	<0.001	<0.001	0.35	0.113	<0.001	<0.001	<0.001	99.48	0.03	<0.001
	G-3-12-5	192.33	524.50	0.01424	<0.001	<0.001	<0.001	0.33	0.094	<0.001	<0.001	<0.001	99.55	0.02	<0.001
	G-3-17-5	168.00	692.50	0.009	<0.001	<0.001	<0.001	0.266	0.068	<0.001	<0.001	<0.001	99.63	0.02	0.003
	G-3-21-5	194.42	886.92	0.013	<0.001	<0.001	<0.001	0.323	0.091	<0.001	<0.001	<0.001	99.55	0.03	<0.001
	G-3-26-5	146.33	1033.25	0.015	<0.001	<0.001	<0.001	0.257	0.072	<0.001	<0.001	<0.001	99.64	0.02	<0.001
	G-3-31-5	165.83	1199.08	0.012	<0.001	<0.001	<0.001	1.171	0.299	<0.001	<0.001	<0.001	98.50	0.02	<0.001
	G-3-37-5	164.42	1363.50	0.012	<0.001	<0.001	<0.001	0.271	0.082	<0.001	<0.001	<0.001	99.62	0.02	<0.001
	G-3-45-5	263.42	1626.92	0.013	<0.001	<0.001	<0.001	0.380	0.096	<0.001	<0.001	<0.001	99.49	0.02	<0.001

Table A.14. Percent Composition of Gas in Samples – Dry CST, 25°C, Thermal System

| Sample | Laboratory ID | Δ Time (hr) | Cumulative Run Time (hr) | Mole Percent Gas, 25 °C | | | | | | | | | | | |
				H_2	He-3	He	CH_4	N_2	O_2	Ne	C_2H_6	CO	Ar	CO_2 /N_2O	Other HC
Test 2, Vessel 2-3	G-2-158-3	123.00	123.00	0.016	<0.001	<0.001	<0.001	1.50	0.397	<0.001	<0.001	<0.001	98.05	0.03	<0.001
	G-3-3-3	209.17	332.17	0.013	<0.001	<0.001	0.006	7.85	2.07	<0.001	<0.001	<0.001	90.0	0.04	0.003
	G-3-12-3	192.33	524.50	0.013	<0.001	0.020	<0.001	0.197	0.058	<0.001	<0.001	<0.001	99.69	0.02	<0.001
	G-3-17-3	168.00	692.50	0.015	<0.001	<0.001	<0.001	0.115	0.033	<0.001	<0.001	<0.001	99.81	0.03	<0.001
	G-3-21-3	194.42	886.92	0.018	<0.001	<0.001	<0.001	0.113	0.028	<0.001	<0.001	<0.001	99.82	0.02	<0.001
	G-3-26-3	146.33	1033.25	0.011	<0.001	<0.001	<0.001	0.098	0.035	<0.001	<0.001	<0.001	99.83	0.02	<0.001
	G-3-31-3	165.83	1199.08	0.015	<0.001	<0.001	<0.001	0.124	0.040	<0.001	<0.001	<0.001	99.79	0.03	<0.001
	G-3-37-3	164.42	1363.50	0.012	<0.001	<0.001	<0.001	0.119	0.048	<0.001	<0.001	<0.001	99.80	0.02	<0.001
	G-3-45-3	263.42	1626.92	0.011	<0.001	<0.001	0.006	8.5	2.26	<0.001	<0.001	<0.001	89.20	0.04	<0.001
Test 2, Vessel 2-7	G-2-158-7	123.00	123.00	0.012	<0.001	<0.001	<0.001	1.44	0.371	<0.001	<0.001	<0.001	98.15	0.03	<0.001
	G-3-3-7	209.17	332.17	0.015	<0.001	<0.001	<0.001	0.47	0.129	<0.001	0.006	<0.001	99.35	0.03	<0.001
	G-3-12-7	192.33	524.50	0.012	<0.001	<0.001	<0.001	0.184	0.045	<0.001	<0.001	<0.001	99.73	0.03	<0.001
	G-3-17-7	168.00	692.50	0.011	<0.001	<0.001	<0.001	0.108	0.032	<0.001	<0.001	<0.001	99.82	0.02	<0.001
	G-3-21-7	194.42	886.92	0.013	<0.001	<0.001	<0.001	0.087	0.026	<0.001	0.004	<0.001	99.85	0.02	<0.001
	G-3-26-7	146.33	1033.25	0.014	<0.001	<0.001	<0.001	0.086	0.028	<0.001	<0.001	<0.001	99.85	0.02	<0.001
	G-3-31-7	165.83	1199.08	0.012	<0.001	<0.001	<0.001	0.162	0.052	<0.001	<0.001	<0.001	99.75	0.02	<0.001
	G-3-37-7	164.42	1363.50	0.011	<0.001	<0.001	<0.001	0.082	0.027	<0.001	<0.001	<0.001	99.86	0.02	<0.001
	G-3-45-7	263.42	1626.92	0.010	<0.001	<0.001	<0.001	0.105	0.037	<0.001	<0.001	<0.001	99.82	0.02	<0.001

Table A.15. Percent Composition of Gas in Samples – Simulant w/ TOC + CST, 25°C, Thermal System

| Sample | Laboratory ID | Δ Time (hr) | Cumulative Run Time (hr) | Mole Percent Gas, 25 °C | | | | | | | | | | | |
				H_2	He-3	He	CH_4	N_2	O_2	Ne	C_2H_6	CO	Ar	CO_2 /N_2O	Other HC
Test 2, Vessel 2-2	G-2-158-2	123.00	123.00	0.016	<0.001	<0.001	<0.001	0.459	0.153	<0.001	<0.001	<0.001	99.34	0.02	0.003
	G-3-3-2	209.17	332.17	0.013	<0.001	<0.001	<0.001	0.156	0.072	<0.001	<0.001	<0.001	99.74	0.02	<0.001
	G-3-12-2	192.33	524.50	0.013	<0.001	<0.001	<0.001	0.166	0.064	<0.001	<0.001	<0.001	99.74	0.02	<0.001
Test 2, Vessel 2-6	G-2-158-6	123.00	123.00	0.014	0.022	<0.001	<0.001	0.271	0.099	<0.001	<0.001	<0.001	99.56	0.03	0.003
	G-3-3-6	209.17	332.17	0.016	<0.001	<0.001	<0.001	0.156	0.069	<0.001	<0.001	<0.001	99.728	0.03	<0.001
	G-3-12-6	192.33	524.50	0.011	<0.001	<0.001	<0.001	0.139	0.049	<0.001	<0.001	<0.001	99.78	0.02	<0.001

Table A.16. Percent Composition of Gas in Samples – Simulant w/ TOC + CST, 70°C, Thermal System

| Sample | Laboratory ID | Δ Time (hr) | Cumulative Run Time (hr) | Mole Percent Gas, 25 °C | | | | | | | | | | | |
				H_2	He-3	He	CH_4	N_2	O_2	Ne	C_2H_6	CO	Ar	CO_2 /N_2O	Other HC
Test 2, Vessel 2-4	G-2-158-4	123.00	123.00	0.013	<0.001	<0.001	<0.001	0.46	0.056	<0.001	<0.001	<0.001	99.43	0.03	<0.001
	G-3-3-4	209.17	332.17	0.015	<0.001	<0.001	0.007	8.9	2.29	<0.001	0.006	<0.001	88.7	0.1	0.003
	G-3-12-4	192.33	524.50	0.014	<0.001	<0.001	0.005	0.170	0.040	<0.001	<0.001	<0.001	99.93	0.04	<0.001
Test 2, Vessel 2-8	G-2-158-8	123.00	123.00	0.014	<0.001	<0.001	<0.001	0.42	0.038	<0.001	0.007	<0.001	99.49	0.026	<0.001
	G-3-3-8	209.17	332.17	0.013	<0.001	<0.001	<0.001	0.143	0.031	<0.001	0.007	<0.001	99.7	0.1	<0.001
	G-3-12-8	192.33	524.50	0.015	<0.001	<0.001	<0.001	0.140	0.028	<0.001	<0.001	<0.001	99.8	0.1	<0.001

Appendix B – TSCR Column Dose Modeling

The gas generation testing described in this report was conducted using a Co-60 source that had a known activity of approximately 2500 Ci. During experimental planning, it was proposed that an independent estimation of the expected dose rate would be a valuable comparison with the experimental dose rate. In this appendix, the inputs and methods used to estimate the absorbed dose in crystalline silicotitanate (CST) media based on the Tank Side Cesium Removal (TSCR) system column geometry are described. The dose estimate was generated using conservative assumptions of maximum activity loading and process fluids present; from these conservative inputs an estimate of dose was generated using Monte Carlo N-Particle (MCNP®), Version 6.2[1]. For simplicity, instances of MCNP that appear in this appendix refer to this version even though it is not included with the acronym. The highest total dose rate (across a range of assumed fluid densities) produced from the MCNP model exercise was $4.85 \times 10^8 \pm 1.94 \times 10^5$ Rad over a 60-day period, or a nominal rate of 336.6 ± 0.1 krad/hr. The stated uncertainty is based on a 95% confidence interval (2σ).

B.1 Quality Assurance of MCNP Model

The MCNP dose modeling results were generated in accordance with the requirements of procedure PNL-MA-870 AP-17, *Radiation Measurements and Irradiations (RMI) NQA-1 Design Control*. Computational results were obtained using the MCNP code, which was not verified and validated for use under the QA program described in Section 2.0, "Quality Assurance". Therefore, even though the model was run in a manner consistent with PNNL procedures and best practices, the model results described in this appendix are considered for-information-only (FIO) and should be treated as such.

B.2 Model Inputs

In this subsection, all the various inputs required to execute the MCNP model are specified as they were used in the calculation. When possible, the source of the input is included. The model was built using the best-known information regarding the TSCR column geometry shown below in Figure B.1. In this section, the various model inputs are discussed, including the process fluid properties (Section B.2.1), CST properties (Section B.2.2), column geometry and materials (Section B.2.3), constants used (Section B.2.4), and governing assumptions (Section B.2.5).

---

[1] Both Monte Carlo N-Particle and MCNP® are registered trademarks owned by Triad National Security, LLC. For more information, see https://mcnp.lanl.gov/.
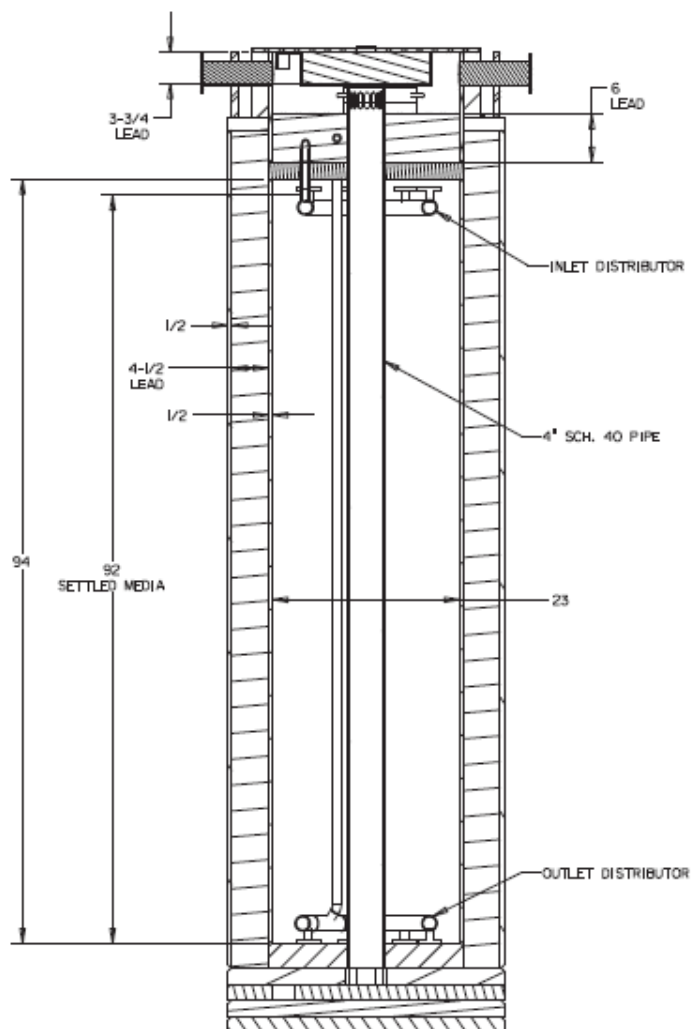
Figure B.1. Cross-section schematic of planned TSCR column used to establish MCNP model geometric parameters.[1]

B.2.1 Process Fluid Inputs

The process fluid was assumed, compositionally, to be 100% water. However, despite specifying the process fluid as water, the liquid density was assumed to span a range of process fluid/CST mass fractions. The initial model runs were performed using a density of 1.21 g/mL, which was based on available data for AP-107 from the Tank Waste Information Network System.[2] More recent measurements of AP-107 tank waste supernatant density (the first planned feed to the TSCR system) were subsequently performed. In Rovira et al. (2018), the density of AP-107 is reported as 1.27 g/mL. The lower bound on liquid density was taken to be that of water, nominally 1.00 g/mL. The process fluid

---

[1] In an e-mail from Matthew R. Landon (WRPS) to Philip P. Schonewill (PNNL) on September 19, 2018, titled *"FW: 30% design review,"* WRPS provided PNNL with a draft drawing "H-14-111250 Rev. A Sheet 1.pdf." This schematic is a portion of that drawing.

[2] https://twinsweb.labworks.org/twinsdata/Forms/About.aspx?subject=TWINS, accessed June 5, 2018.

(liquid) density, ρ_{liq}, determines the mass ratio between the CST and fluid phase. To establish the impact of the CST/fluid mass ratio, the model was run using both $\rho_{liq} = 1.00$ g/mL and $\rho_{liq} = 1.27$ g/mL.

Air is also present outside the column and in the column annulus. Thus, it is also a relevant process fluid to include in the model. Air is specified as having the composition given in Table B.1, with a density of 0.001205 g/mL (McConn Jr et al. 2011). Note the term ZAID is specific to MCNP and refers to the "element (Z) and isotope (A) portion" of an ID number that uniquely identifies an atomic cross-section (neutron or photon) in the model. They are provided for completeness so another MCNP user could duplicate the model.

Table B.1. Air inputs for MCNP model.

Element	Element Cross-Section (ZAID)	Weight Fraction
C	6000	0.000124
N	7014	0.755268
O	8016	0.231781
Ar	18000	0.012827

B.2.2   CST Inputs

The CST composition was taken be $Na_2(H_2O)_2Ti_4O_5(OH)(SiO_4)_2Na(H_2O)_{1.7}$ (see Fondeur et al. 2000). This composition is an approximation based on information available in literature, because the CST composition is proprietary (for example, it includes some niobium substituted for the titanium shown in the composition above). For additional discussion of this topic, refer to Pease et al. (2019).

The bed porosity (ε_{bed}) and CST particle porosity (ε_p) were assumed to be 0.50 and 0.24, respectively. These values are given by Hamm et al. (2002). The CST particle density (ρ_p) is quoted by Hamm et al. as being 2.6 g/mL. Using these parameters, the saturated (wet) bed density can be calculated as shown in Section B.2.2.1. Once the wet bed density and mass ratio of CST to liquid are known, the wet CST slurry composition can be formulated as described in Section B.2.2.2.

B.2.2.1   Calculation of Wet Resin Density

The density of the dry CST bed, based on bed volume, is defined as

$$\rho_{dbed} = \frac{m_{CST}}{V_{bed}} = \rho_p \left[1 - \left\{ \varepsilon_{bed} + \left(1 - \varepsilon_{bed} \right) \varepsilon_p \right\} \right]$$

where m_{CST} is the mass of CST and V_{bed} is the volume of the bed. This accounts for both the internal pore volume of the CST particles and the bed pore volume (voids between CST particles). The quantity enclosed in curly brackets is the total porosity of the system, ε_T.

Using the values given in Section B.2.2, $\rho_{dbed} \sim 0.988$ g CST/mL bed. This is consistent with the commonly quoted value of 1.0 g/mL for this quantity. For any given bed volume, assuming that the entire void space represented by the total porosity is filled with liquid, there is an equivalent amount of liquid, i.e.,

$$\frac{m_{liq}}{V_{bed}} = \varepsilon_T \rho_{liq}$$

where m_{liq} and ρ_{liq} are the mass and density of the interstitial liquid, respectively. For the liquid of interest, ρ_{liq} ranges between 1.00 to 1.27 g/mL (Section B.2.1) and $m_{liq}/V_{bed} = 0.620$ to 0.787 g liquid/mL bed.

Thus, each unit of volume contains 0.988 g of CST and between 0.620 and 0.787 g of liquid by this calculation. The resulting mass ratios are between 61.4% CST and 38.6% liquid (ρ_{liq} of 1.00 g/mL) and 55.6% CST and 44.3% liquid (ρ_{liq} of 1.27 g/mL). The bulk (wet) density of the bed can be estimated as

$$\rho_{bulk} = \varepsilon_T \rho_{liq} + (1 - \varepsilon_T) \rho_p$$

Using the values calculated above, the bulk density (ρ_{bulk}) ranges from 1.61 to 1.78 g/mL. These values were used for the wet CST media bed density in the MCNP calculation.

B.2.2.2 CST Material Composition Input for MCNP Model

Using the chemical formula of CST, the weight percentage of each of the elements that make up the CST media can be generated. The elemental mass of the CST material is listed in Table B.2. The total molar mass for CST (MW$_{CST}$) is 608.34 g/mol.

Table B.2. CST resin elemental mass.

Element	Number of Atoms	Molar Mass (g/mol)	Total Mass of Each Element (g/mol CST)
Na	2	22.99	45.98
H	4	1.008	4.03
O	2	16.00	32.00
Ti	4	47.88	191.52
O	5	16.00	80.00
O	1	16.00	16.00
H	1	1.008	1.01
Si	2	28.09	56.18
O	8	16.00	128.00
Na	1	22.99	22.99
H	3.4	1.008	3.43
O	1.7	16.00	27.20
Total Molar Mass (g/mol)			608.34

During normal operation, the CST media in the bed will be immersed in waste supernate (such as AP-107). In this model, the supernate is assumed to be water regardless of the liquid density used to calculate

the mass ratios. While other constituents are in the stream, it is assumed that these other species will escape the column and only the liquid water will remain.

In Section B.2.2.1 the portion of the column occupied by the CST (f_{CST}) and the liquid portion (f_{liq}) were calculated for the two bounding liquid densities. Using these values, the total mass fraction x of each element i can be calculated via the following expression:

$$x_i = f_{CST} \frac{n_{i,CST} MW_i}{MW_{CST}} + f_{liq} \frac{n_{i,liq} MW_i}{MW_{liq}},$$

where $n_{i,CST}$ and $n_{i,liq}$ are the number of molecules of element i in each phase, respectively, MW_i is molar mass of element i, and MW_{CST} and MW_{liq} are the total molar mass of the CST and liquid (water) phases, respectively. The mass fraction distribution for the two density extremes is shown in Table B.3.

Table B.3. Wet CST elemental composition used in the MCNP model.

Element	Element Cross-Section (ZAID)	Weight Fraction x_i Used in MCNP (ρ_{liq} = 1.27 g/mL)	Weight Fraction x_i Used in MCNP (ρ_{liq} = 1.00 g/mL)
O	8016	0.6529	0.6285
H	1000	0.0574	0.0517
Na	11000	0.0631	0.0697
Ti	22000	0.1752	0.1934
Si	14000	0.0514	0.0567

B.2.3   Column Materials and Dimensions

The TSCR column materials of interest are 316L stainless steel and lead. The stainless steel composition (see Table B.4) was specified by following the composition information provided by McConn Jr et al. (2011). McConn Jr et al. also reports the density of stainless steel as 8.00 g/mL. Lead was assumed to be elemental (mass fraction = 1.0) with no impurities; the lead element's ZAID is 82000. Lead has a density of 11.35 g/mL (McConn Jr et al. 2011).

Table B.4. 316L stainless steel composition used in the MCNP model.

Element	Element Cross-Section (ZAID)	Weight Fraction
C	6000	0.00041
Si	14000	0.00507
P	15000	0.00023
S	16000	0.00015
Cr	24000	0.17000
Mn	25000	0.01014
Fe	26000	0.66900
Ni	28000	0.12000
Mo	42000	0.02500

The CST column was modeled using the geometric parameters given in Table B.5. The parameters were developed from the dimensions provided in Figure B.1. The geometric model was simplified by ignoring the distributors at the top and bottom of the column and assuming the entire annular region was filled with the wet CST bed.

Table B.5. Column geometric parameters used in the MCNP model.

Cs Column Name	Dimension (in.)
Stainless Wall Thickness	0.50
Inner Diameter of Air Annulus	23.00
Pressure Vessel Outer Diameter	33.00
Pressure Vessel Footing Outer Diameter	55.00
Lead Shielding Around Vessel Thickness	5.00
CST Resin Height	92.00
Height of Lead Side Shielding	94.00
Lead Top Plug	6.00
Lead Base Thickness	2.00

B.2.4   Conversion and Emission Factors

For gamma emission, Cs-137 emits 9.318×10^{-1} photons/decay, which is actually produced from its daughter product Ba-137m (Browne and Firestone 1986). Thus, the gamma emission factor is 0.9318. Cs-137 decays by beta particle emission 100% of the time (National Nuclear Data Center Table of Nuclides[1]), represented by a beta emission factor of 1.0. Table B.6 shows the other conversion factors used in the model and their sources (reference).

Table B.6. Conversion factors used in the model.

Convert From	Convert To	Multiply By	Reference
Joule (J)	Electron volt (eV)	$6.241509126 \times 10^{18}$	NIST[a]
Gram (g)	Kilogram (kg)	0.001	Commonly Known Conversion
Milliliters (mL)	Cubic centimeters (cm^3)	1	Commonly Known Conversion
Joule/kilogram (J/kg)	Gray (Gy)	1	Health Physics Society (HPS)[b]
Gray (Gy)	Rad	100	HPS[b]
Curie (Ci)	Becquerel (Bq)	3.7×10^{10}	HPS[c]

(a) The National Institute of Standards and Technology (NIST) Reference on Constants, Units, and Uncertainties, https://physics.nist.gov/cuu/Constants/index.html, accessed June 5, 2018.
(b) Gray (Gy), http://hps.org/publicinformation/radterms/radfact79.html, accessed June 5, 2018.
(c) Curie (Ci), http://hps.org/publicinformation/radterms/radfact50.html, accessed June 5, 2018.

---

[1] Chart of Nuclides, https://www.nndc.bnl.gov/chart/reCenter.jsp?z=55&n=82, accessed June 5, 2018.

The emission factors were used to build a tally multiplier to convert the F6 results (given in megaelectronvolts (MeV) g^{-1}) into units of MeV g^{-1} d^{-1} Ci^{-1} in order to compute the MeV on a per-day, per-curie basis. The construction of the tally multiplier for beta and gamma cases is given in Table B.7.

Table B.7. Tally multiplier for F6 results.

Case	Bq per Ci	Emission Factor	Hours per Day	Seconds per Hour	Conversion Factor (disintegrations × d × Ci)
Beta	3.70×10^{10}	1.0	24	3600	3.20×10^{15}
Photon	3.70×10^{10}	0.9318	24	3600	2.98×10^{15}

B.2.5 Governing Assumptions

The assumptions that govern the construction of the model are provided in the enumerated list below. Each assumption has a short description and a justification for why the assumption is thought to be conservative.

1. **Loading of cesium in the CST bed is assumed to be uniform.**

   For MCNP modeling purposes it is most straightforward to assume that the cesium is distributed evenly through the column. While initially the column may load in the direction of waste flow, over time as receptor locations fill up, the loading should become more uniform.

2. **Other constituents from the waste stream do not absorb onto the CST bed.**

   There is marginal benefit in including the fractional amounts of other constituents in the wet CST composition system. They are not likely to contribute significantly to the outcome.

3. **The maximum loading (150,000 Ci) of cesium is assumed to occur instantaneously.**

   This is a very conservative assumption, because the cesium will be loaded gradually over the course of several days. The assumed maximum loading also may not be achieved during normal processing due to interferences from other constituents.

4. **The column remains in the maximum loaded condition for a period of 60 days.**

   The CST columns are not likely to remain in contact with process fluid for a period as long as 60 days, which is approximately twice the expected waste loading period. This generates a total dose estimate for a period of time similar to the gas generation testing. The dose rate is constant and irrespective of the assumed duration.

5. **Column geometric dimensions that are not well known can be replaced with reasonable estimates.**

   The spacer plate above the column is assumed to be a 1 in. plate made of 316L stainless steel. The base plate is assumed to be 2 in. of lead following by 4 in. of 316L stainless steel. The annular pipe is also assumed to be 316L stainless steel.

The assumed materials and dimensions are reasonable and conservative for the problem. Including material above and below the CST bed rather than leaving it out of the model increases the potential for backscatter, which increases dose.

B.3 Results

The MCNP calculation was performed using the two input files (or similar versions thereof) provided in Section B.4. The example input files show the model run with an assumed liquid density of 1.00 g/mL (bulk density of 1.61 g/mL). Model runs with other liquid densities have the same formulation except the input values affected by the liquid density (and bulk density) were adjusted appropriately. In each model case, 10 out of 10 statistical tests applied to the model run were passed. The model performs an F6 tally, which provides the result in units of MeV g^{-1}. The tally multipliers of the model are used to translate the results into units of MeV g^{-1} d^{-1} Ci^{-1}, which are presented in Table B.8. The tally results are used in conjunction with the conversion factors in Section B.2.4 and the assumed duration (60 days) and loading (150,000 Ci) to compute the total dose in units of rad. The final dose values derived from the results are also shown in Table B.8.

Table B.8. Final dose result generated from MCNP6.2 (Mode P,E) run tally values.

Case Description and Related Input File	MCNP6.2 F6 Tally Result (MeV g^{-1} d^{-1} Ci^{-1})	Relative Tally Error (MeV g^{-1} d^{-1} Ci^{-1})	Uncertainty in Tally Error[a]	Total Dose (rad)	Uncertainty in Total Dose[a] (rad)
ρ_{liq} = 1.00 g/mL, Photon Decay (Gamma)	2.74×10^9	2.00×10^{-4}	1.10×10^6	3.95×10^8	1.58×10^5
ρ_{liq} = 1.00 g/mL, Beta Decay from Cs-137	6.21×10^8	2.00×10^{-4}	2.49×10^5	8.96×10^7	3.58×10^4
			Dose Sum	4.85×10^8	1.94×10^5
ρ_{liq} = 1.27 g/mL, Photon Decay (Gamma)	2.56×10^9	2.00×10^{-4}	1.03×10^6	3.70×10^8	1.48×10^5
ρ_{liq} = 1.27 g/mL, Beta Decay from Cs-137	5.62×10^8	2.00×10^{-4}	2.25×10^5	8.10×10^7	3.24×10^4
			Dose Sum	4.51×10^8	1.80×10^5

(a) Assumes a Gaussian distribution at the 95% confidence level (2σ) for an infinitely large number of model realizations.

Although a series of other model runs could be used to generate data in the same way as the example shown in Table B.8, the two density cases are sufficient to get an order-of-magnitude approximation of the dose in this type of system. The total dose results range from 4.85×10^8 (ρ_{liq} = 1.00 g/mL. ρ_{bulk} = 1.61 g/mL) to 4.51×10^8 (ρ_{liq} = 1.27 g/mL. ρ_{bulk} = 1.78 g/mL) rad. Table B.9 summarizes the total dose obtained for each density, the uncertainty generated at the 95% confidence level, and the hourly dose rate assuming the total dose occurs uniformly over the 60-day duration.

Table B.9. Summary of MCNP model results and nominal dose rates.

Liquid Density, g/mL	Bulk (Wet Bed) Density, g/mL	Total Dose, rad	Uncertainty in Total Dose, rad	Nominal Dose Rate, krad/hr	Uncertainty in Nominal Dose Rate, krad/hr
1.00	1.61	4.85×10^8	1.94×10^5	336.6	0.1
1.27	1.78	4.51×10^8	1.80×10^5	313.1	0.1

B.4 Example MCNP Files

This section includes example input files used to model photons (gamma) from Ba-137m, a daughter of Cs-137, and beta from Cs-137. The photon input file is given in Section B.4.1, and the beta input file in Section B.4.2.

B.4.1   MCNP Input File – Photons from Ba-137m

```
Absorption Vessel, Version 3
c Built by M Conrady, 06/13/2019
c Cs-137 loading up to Max of 150,000 Ci
c Absorbed dose result is 1 Ci for 1 day of Cs137
c This input models the photons emitted from Ba137m. Dose includes betas and photons.
c Cell Cards
1 1 -8.00 -2 1 -13 imp:p,e=1 $ Steel Base of Column
2 2 -11.35 -3 14 2 -11 imp:p,e=1 $ Lead in Base of Column
3 4 -1.61 -4 14 3 -10 imp:p,e=1 $ CST
4 3 -0.001205 -5 4 -10 14 imp:p,e=1 $ Air Gap Above CST
5 1 -8.00 -6 14 5 -11 imp:p,e=1 $ SS Separator Plate
6 1 -8.00 -5 3 -11 10 imp:p,e=1 $ SS Inner Wall
7 2 -11.35 -12 11 -7 2 imp:p,e=1 $ Lead Shield Walls
8 1 -8.00 -13 12 -7 2 imp:p,e=1 $ SS Outer Wall
9 2 -11.35 -10 14 -7 6 imp:p,e=1 $ Top Lead Shield
10 1 -8.00 -14 15 -7 2 imp:p,e=1 $ 4" Sch. 40 Pipe
11 3 -0.001205 -15 -7 2 imp:p,e=1 $ Air Inside 4" Sch. 40 Pipe
12 1 -8.00 -7 6 -11 10 imp:p,e=1 $ SS Wall Extensions Around Upper Lead Shield
100 0 -1:7:13 imp:p,e=0
c Blank Line Follows

c Surface Cards
1 pz 0 $ Origin
2 pz 10.16 $ Base of Column
3 pz 15.24 $ Lead in Base of Column
4 pz 248.92 $ Height of CST Media
5 pz 254.00 $ Height of Column Outer Walls
6 pz 256.54 $ Top of SS Separator Plate
7 pz 271.78 $ Top of Lead Shield
c
10 cz 29.21 $ Inner Radius of Column
11 cz 30.48 $ Outer Radius of Inner SS Wall
12 cz 41.91 $ Outer Radius of Lead Shield Wall
13 cz 43.18 $ Outer Radius of Outer SS Wall
14 cz 5.715 $ Outer Radius of 4" Pipe
15 cz 5.14096 $ Inner Radius of 4" Pipe
c Blank Card Follows

c Data Cards
c Material 1 is 316L Stainless Steel, Material 300, PNNL-15870, Rev. 1, rho=8.00 g/cc
m1 6000 -0.000410
```

```
 14000 -0.005070
 15000 -0.000230
 16000 -0.000150
 24000 -0.170000
 25000 -0.010140
 26000 -0.669000
 28000 -0.120000
 42000 -0.025000
c
c Material 2 is lead, Material 171, PNNL-15870, Rev. 1, rho=11.35 g/cc
m2 82000 -1.00
c
c Material 3 is Air (Dry, Near Sea Level), Material 4, PNNL-15870, Rev. 1, rho=0.001205 g/cc
m3 6000 -0.000124
 7000 -0.755268
 8000 -0.231781
 18000 -0.012827
c
c Material 4 is Wet CST, rho=1.00 g/cc for liquid, bed density is 1.61 g/cc
m4 11000 -0.069660206
 1000 -0.05170049
 8000 -0.628460488
 22000 -0.193436604
 14000 -0.056742212
c
c Cs-137, 1 Ci, 0 s old, TORI-86 Library
c Total rate = 9.318E-1 photons/decay
c = 3.448E4 photons/(s uCi)
c 1 Ci for 1 Day emits 2.98E15 photons
c Energy Branching
c (MeV) Fraction
# si3 sp3
 L D
 0.003954 1.436E-4 $ Cs-137
 0.004331 6.447E-5 $ Cs-137
 0.004465 3.983E-3 $ Cs-137
 0.004944 3.658E-3 $ Cs-137
 0.005620 4.878E-4 $ Cs-137
 0.031817 2.050E-2 $ Cs-137
 0.032194 3.774E-2 $ Cs-137
 0.036357 1.044E-2 $ Cs-137
 0.037450 2.643E-3 $ Cs-137
 0.661660 8.521E-1 $ Cs-137
c End Cs-137
c
sdef cel=3 pos=0 0 30.48 rad=d1 erg=d3 ext=d4 axs=0 0 1 par=2
si1 H 10.16 29.21
sp1 0 1
si4 0 264.16
c
mode p e
c
F6:p,e 3
FM6 2.98E15
nps 5E6
rand gen=2 stride=137892567
print
```

B.4.2   MCNP Input File – Beta Emissions from Cs-137

```
Absorption Vessel, Version 3
c Built by M Conrady, 06/13/2019
c Cs-137 loading up to Max of 150,000 Ci
c Absorbed dose result is 1 Ci for 1 day of Cs137
c This input models the betas emitted from Cs137. Dose includes betas and photons.
c Cell Cards
1 1 -8.00 -2 1 -13 imp:p,e=1 $ Steel Base of Column
2 2 -11.35 -3 14 2 -11 imp:p,e=1 $ Lead in Base of Column
3 4 -1.61 -4 14 3 -10 imp:p,e=1 $ CST
4 3 -0.001205 -5 4 -10 14 imp:p,e=1 $ Air Gap Above CST
5 1 -8.00 -6 14 5 -11 imp:p,e=1 $ SS Separator Plate
6 1 -8.00 -5 3 -11 10 imp:p,e=1 $ SS Inner Wall
7 2 -11.35 -12 11 -7 2 imp:p,e=1 $ Lead Shield Walls
8 1 -8.00 -13 12 -7 2 imp:p,e=1 $ SS Outer Wall
9 2 -11.35 -10 14 -7 6 imp:p,e=1 $ Top Lead Shield
10 1 -8.00 -14 15 -7 2 imp:p,e=1 $ 4" Sch. 40 Pipe
11 3 -0.001205 -15 -7 2 imp:p,e=1 $ Air Inside 4" Sch. 40 Pipe
12 1 -8.00 -7 6 -11 10 imp:p,e=1 $ SS Wall Extensions Around Upper Lead Shield
100 0 -1:7:13 imp:p,e=0
c Blank Line Follows

c Surface Cards
1 pz 0 $ Origin
2 pz 10.16 $ Base of Column
3 pz 15.24 $ Lead in Base of Column
4 pz 248.92 $ Height of CST Media
5 pz 254.00 $ Height of Column Outer Walls
6 pz 256.54 $ Top of SS Separator Plate
7 pz 271.78 $ Top of Lead Shield
c
10 cz 29.21 $ Inner Radius of Column
11 cz 30.48 $ Outer Radius of Inner SS Wall
12 cz 41.91 $ Outer Radius of Lead Shield Wall
13 cz 43.18 $ Outer Radius of Outer SS Wall
14 cz 5.715 $ Outer Radius of 4" Pipe
15 cz 5.14096 $ Inner Radius of 4" Pipe
c Blank Card Follows

c Data Cards
c Material 1 is 316L Stainless Steel, Material 300, PNNL-15870, Rev. 1, rho=8.00 g/cc
m1 6000 -0.000410
 14000 -0.005070
 15000 -0.000230
 16000 -0.000150
 24000 -0.170000
 25000 -0.010140
 26000 -0.669000
 28000 -0.120000
 42000 -0.025000
c
c Material 2 is lead, Material 171, PNNL-15870, Rev. 1, rho=11.35 g/cc
m2 82000 -1.00
c
c Material 3 is Air (Dry, Near Sea Level), Material 4, PNNL-15870, Rev. 1, rho=0.001205 g/cc
m3 6000 -0.000124
 7000 -0.755268
 8000 -0.231781
 18000 -0.012827
c
c Material 4 is Wet CST, rho=1.00 g/cc for liquid, bed density is 1.61 g/cc
m4 11000 -0.069660206
 1000 -0.05170049
```

```
 8000 -0.628460488
 22000 -0.193436604
 14000 -0.056742212
c
c Cs-137, 1 Ci, 0 s old, TORI-86 Library
c Total rate = 1 beta/decay
c = 3.7E4 photons/(s uCi)
c 1 Ci for 1 Day emits 3.20E15 betas
c Energy Branching
c (MeV) Fraction
# si3 sp3
 L D
 0.0294 1.93E-01 $ Cs-137
 0.0880 1.76E-01 $ Cs-137
 0.1467 1.61E-01 $ Cs-137
 0.2053 1.43E-01 $ Cs-137
 0.2640 1.22E-01 $ Cs-137
 0.3227 9.38E-02 $ Cs-137
 0.3813 6.01E-02 $ Cs-137
 0.4400 2.64E-02 $ Cs-137
 0.4986 5.70E-03 $ Cs-137
 0.5573 3.30E-03 $ Cs-137
 0.6160 3.07E-03 $ Cs-137
 0.6746 2.82E-03 $ Cs-137
 0.7333 2.53E-03 $ Cs-137
 0.7919 2.20E-03 $ Cs-137
 0.8506 1.83E-03 $ Cs-137
 0.9093 1.42E-03 $ Cs-137
 0.9679 9.92E-04 $ Cs-137
 1.0266 5.91E-04 $ Cs-137
 1.0852 2.45E-04 $ Cs-137
 1.1439 5.38E-05 $ Cs-137
c End Cs-137
c
sdef cel=3 pos=0 0 30.48 rad=d1 erg=d3 ext=d4 axs=0 0 1 par=3
si1 H 10.16 29.21
sp1 0 1
si4 0 264.16
c
mode p e
c
F6:p,e 3
FM6 3.20E15
nps 2E7
rand gen=2 stride=137892567
print
```
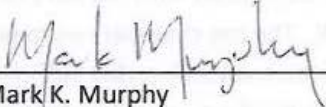
B.5 References

Browne E and RB Firestone. 1986. "Table of Radioactive Isotopes," New York: John Wiley & Sons.

Fondeur FF, CV Philip, and RG Anthony. 2000. *Crystalline Silicotitanate Ion Exchange Support for Salt Alternatives*. SRT-LWP-2000-00189, Westinghouse Savannah River Company, Aiken, South Carolina.

Hamm LL, T Hang, DJ McCabe, and WD King. 2002. *Preliminary Ion Exchange Modeling for Removal of Cesium from Hanford Waste Using Hydrous Crystalline Silicotitanate Material*. WSRC-TR-2001-00400, Westinghouse Savannah River Company, Aiken, South Carolina.

McConn Jr RJ, CJ Gesh, RT Pagh, RA Rucker, and RG Williams III. 2011. *Compendium of Material Composition Data for Radiation Transport Modeling*. PNNL-15870, Rev. 1 (PIET-43741-TM-963). Pacific Northwest National Laboratory, Richland, Washington.

Pease LF, SK Fiskum, HA Colburn, and PP Schonewill. 2019. *Cesium Ion Exchange with Crystalline Silicotitanate: Literature Review*. PNNL-28343, Rev. 0 (RPT-LPTTS-001, Rev. 0). Pacific Northwest National Laboratory, Richland, Washington.

Rovira AM, SK Fiskum, HA Colburn, JR Allred, MR Smoot, and RA Peterson. 2018. *Cesium Ion Exchange Testing Using Crystalline Silicotitanate with Hanford Tank Waste 241-AP-107*. PNNL-27706 (RPT-DFTP-011, Rev. 0). Pacific Northwest National Laboratory, Richland, Washington.
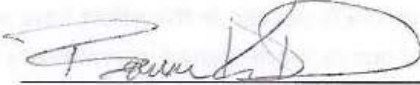
Appendix C – Source Calibration Information

REPORT of CALIBRATION

Client:	Tracking No.:	18284
PNNL Heather Colburn, Sam Bryan LAWPS Technology Transfer Support Project: 72195 PM: Phillip Schonewill	Task:	Calibration of Absorbed Dose Rate to Water within CST and liquid-filled lower half of reaction vessels centered approximately 5.75 cm from Co-60 source.
	Measurement Dates:	July 3, 2018
	Final Report Date:	April 19, 2019

Measurements Performed and Reported by:

Mark Murphy   4/22/2019

Mark K. Murphy   Date
Engineer
Phone: (509)375-7331; Email: mark.murphy@pnnl.gov

Reviewed by:

[signature]   4/22/2019

Roman K. Piper   Date
Engineer
Phone: (509)375-7339; Email: kim.piper@@pnnl.gov

Colburn Gamma Bunker dose characterization 24Apr2019 signed.docx   April 21, 2019

Overview:

This report provides a summary of the dose and dose rate values resulting from measurements conducted on July 3, 2018 within steel "gas reaction vessels" positioned within the 318 building *Gamma Bunker,* while ^{60}Co source 318-528 (2700 curies at that time) was in loaded position. These measurements were obtained using two methods – *air ionization chamber* and *photo-fluorescent film*. Measurements were conducted in four gas vessels, as well as an "in air" geometry. The resulting dose rate values were compared to the measured values obtained in January 2016 for ^{60}Co source 318-420 (1170 curies at that time, and a known 2.32X difference in measured dose rate) in order to provide confidence in the values.

Air-Equivalent Ionization Chamber Measurement:

Radiation detectors used to evaluate the exposure rate within the reaction vessels included three Exradin air-equivalent ionization chambers; two Model A12S and one Model A16 with approximate sensitive volumes of 0.24 and 0.007 cm^3, respectively. The Model A12S and A16 ion chambers can be seen in the photos in Figures 1 and 2. The A12S detectors were centered in the vessels at source height, which is 6.75 cm above the inside base of the vessels. The sensitive volume for each A12S was positioned coincident with the cylindrical axis of the vessel volume via the use of custom constructed, low mass plastic spacer rings. Measurements were conducted with the ion chambers placed directly within the vessels, filled with either water or CST fill. The ion chambers were without their respective build-up caps, anticipating that the surrounding medium would provide sufficient charged particle equilibrium (CPE). Calibration of each chamber, with build-up cap applied, was performed prior to these measurements using the 318 Building High Exposure Facility (HEF) ^{60}Co source 318-464. The transfer standard, calibrated at the National Institute of Standards and Technology (NIST), used for these direct replacement measurements was a Capintec Model PM-30, with build-up cap. The equipment listed in Table 1 was used to support these measurements. With the exception of the thermocouple and associated Omega readout listed in the table, all M&TE utilized in this effort have each been calibrated in a manner traceable, via an unbroken chain of one or more related intermediary standards, through (1) recognized standards maintained by the National Institute of Standards and Technology (NIST), (2) other recognized national measurement institutes (NMI), (3) accepted fundamental physical constants, or (4) by specified methods, consensus standards or ratio type measurements.)

The ion chambers were placed within the vessels filled (roughly half-full) with just over 31 mL of either deionized water or CST. This was intended to provide ~14 cm depth (not including chamber displacement).

Temperature monitoring was accomplished using Type K thermocouples (TC) placed within the irradiation chamber. To correct AEIC measurements, the TC placed near the top of the water-filled region was used.

Dose rate to water was determined using the following equation:

$$\dot{D}_w = I_{ioniz} \cdot k_{TP} \cdot k_e \cdot N \cdot k_{D/X} \cdot 3600$$

Colburn Gamma Bunker dose characterization 24Apr2019 signed.docx   April 21, 2019

Where: $\dot{D}_w$ is the average absorbed dose rate to water over the sensitive volume of the AEIC (commonly attributed to the position of the centroid of the chamber), in rad/h,

I_{ioniz} is the measured ionization current, in A (C/s),

k_{TP} is the unitless correction for density of air within the AEIC volume,

k_e is the unitless correction for the readout of the electrometer,

N is the efficiency of each respective AEIC determined through comparison with the secondary transfer standard using the same photon energy, in R/C,

$k_{D/X}$ is the conversion coefficient from exposure (Roentgen) to absorbed dose to water (rad). A value of 0.966 was used, as referenced from ICRU 30 (1979), *Quantitative Concepts and Dosimetry in Radiobiology*,

3600 converts the time interval from seconds to hours.

Table 1: Measuring and Test Equipment			
Device	**S/N**	**Calibration Exp. Date**	**Application/Notes**
AEIC Exradin A16 AIC	XA140585	06/2019	Bunker Vessel Position 6, In Air
AEIC Exradin A12S AIC	XZ151955	06/2019	Bunker Vessel Position 3, in CST
AEIC Exradin A12S AIC	XZ151956	06/2019	Bunker Vessel Position 7, in H_2O
AEIC Capintec PM-30	CII30.7502	7/2018	^{60}Co Transfer Standard used to calibrate Exradin AEICs
Keithley 617 Electrometer	383823	1/2019	Calibration and Bunker measurements (Positions 5 and 7)
Timer	SWFI3-0002	2/2019	Calibration of Exradin AIC charge integration time and for Film irradiation duration.
Thermometer	PTVA1-0001	6/2019	
DigiSense Readout Omega Thermocouple	577785 3197	1/2019	Reaction Vessel in water (Top) – Calibrated against working standard (PTVA1-0001)
Omega Readout Omega Thermocouple	876237 3196	Ind. Only	Reaction Vessel in water (Bottom) (Used only for relative readings)
Barometer	PTVA1-0001	6/2019	
Distance	DRLS1-0003	4/2020	Measuring vessel dimensions and AEIC placement

The central height (6.75 cm above core base) measurement is considered to be the estimate of the traceable absorbed dose rate to water within the volume least affected by geometric conditions (e.g., scatter, stem effects, water/gas interface, etc.) within the volume.

Colburn Gamma Bunker dose characterization 24Apr2019 signed.docx   April 21, 2019

Lithium-Fluoride Film:

The passive dosimetry utilized is the Sunna lithium-fluoride (LiF) film, which is microcrystalline LiF powder within a polyethylene matrix. The film dimensions are 1 cm x 3 cm with a thickness of 0.5 mm. The radiation energy is captured within the LiF storage phosphor, and the fluorescence read out signal (~530 nm, green) is induced by blue excitation light (~440 nm). Depending on the type of readout instrument, the dynamic dose response for the film can range from approximately 2 kGy to 100 kGy or more.

The film measurements were configured within the same type of gas vessels as the AEIC measurements. To allow precise positioning of the films at known height within the gas vessels, the films were stapled to a long, thin plastic strip; and the strip inserted into the gas vessel (See Figure 1). Note that films were stapled on both sides of the PET strip. The film can be placed directly in water for at least 24 hours before water diffusion begins to affect the calibrated emission signal. Given that 4 ½ films were stapled on each side of the PET strip, the region covered by the film extended from the inner base of the vessels to approximately 15.5 cm above the inner base of the vessels; the last ~1 cm likely surrounded by air instead of water.

Films were irradiated during a July 3rd, 2018 measurement run. To ensure the minimum dose to the films was well above the minimum detectable in order to achieve minimal measurement uncertainty, the targeted minimum dose was ~10 kGy. The resulting irradiation duration was 152 minutes, which resulted in the various film locations receiving a range in dose of approximately 10 to 30 kGy.

Although readout of the irradiated dosimeter film was attempted within a few days of the irradiation (using the Perkin-Elmer Model Lambda 600 spectrophotometer), the precision (standard deviation) of the readout values was not near what was required. Due to troubles with the control computer and delays in testing and fabricating a film holder that provided the required position reproducibility, the film readout was delayed until January 2019. The films irradiated within the vessels were analyzed at the same time as a film calibration set (irradiated within hours of the July Gamma Bunker run) in order to account for any post-irradiation change in film signal.

Irradiation Geometry and Procedure:

The photo in Figure 2 shows the irradiation geometry of the gas vessels during the July 2018 measurements. The thin-walled source tube has an OD of 50.0 mm, and the gas vessels (19 mm diameter, 26.9-cm in height, with fill height of ~14 cm) are centered approximately 32.5 mm out from the source tube wall. This resulted in a source center to vessel center distance between 57 and 58 mm. Although some vessels did not have the insulation jacket, the impact on the dose to the center of the vessel was determined to be negligible. Two thermocouples were positioned at top portion of irradiation chamber. After lowering core into the Gamma Bunker, cobalt-60 source 318-528 was loaded

Colburn Gamma Bunker dose characterization 24Apr2019 signed.docx   April 21, 2019

Figure 1: Photos showing LiF film dosimeters stapled to the thin strip of PET with plastic green rings to allow centering within gas vessels (top); a stainless steel gas vessel of 19-mm OD and 26.9-cm length with LiF film assembly inserted (middle); and a Model A12S ionization chamber alongside a gas vessel (bottom). Spacers similar to those holding the film strip centered in the vessel, were also applied to the ion chamber.

for a duration of 152 minutes 5 seconds, during which time readings from the ionization chambers were recorded. The core was lifted, the irradiated films removed, and core lowered again. Cobalt-60 source 318-420 was then loaded and dose rate measurements performed using the ionization chambers. The source 318-420 measurements were performed in order to obtain additional dose rate data for both 318-420 and 318-528 (It is known that the difference between the in-air dose rates is 2.32X; therefore, the source 318-420 data can be corrected to source 318-528).
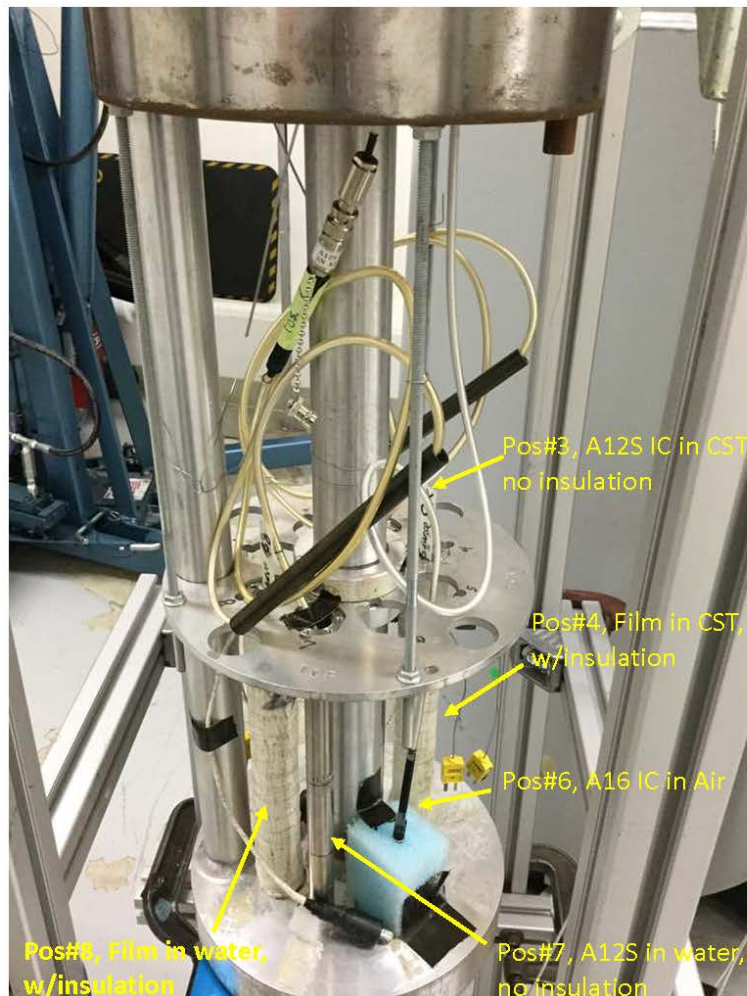
Figure 2: Photo of the gas vessels (insulated and bare) and the Model A16 ionization chamber positioned In-Air within the core of the Gamma Bunker on July 3, 2018. The source center to vessel center distance was verified to be between 57 and 58 mm.

Data Results

Table 2 lists the absorbed dose rate results, relative to water, from the ion chamber and film measurements for the source height position (6.75 cm above core base), for cobalt-60 source 318-528.

Colburn Gamma Bunker dose characterization 24Apr2019 signed.docx   April 21, 2019

Table 2. The dose rate results for July 3, 2018 from the ion chamber and film measurements for the source height position, for cobalt-60 source 318-528.

Bunker Position	Detector	Reaction Vessel Geometry	Surrounding Media	Measured Absorbed Dose Rate Relative to Water (kGy/hr)	
				Source height	volume average*
3	Ion Chamber, 0.24cc	Bare vessel	CST, ~14 cm depth	8.388	6.123
4	Film	Insulated vessel	CST, ~14 cm depth	7.873	5.748
6	Ion Chamber, 0.007cc	No Vessel	Foam, Air	8.415	N/A
7	Ion Chamber, 0.24cc	Bare vessel	Water, ~14 cm depth	8.136	5.939
8	Film	Insulated vessel	Water, ~14 cm depth	7.611	5.556
July 2018 **Ion Chamber** Mean kGy/hr for CST and Water:				**8.26 ± 2.6%	6.03 ±2.6%**
Corrected for **September 2018** Vessel Irradiations:				8.07	**5.88**
Corrected for **January 2019** Vessel Irradiations:				7.68	**5.61**
July 2018 **Film** Mean kGy/hr for CST and Water:				#7.74 ± 13%	5.65 ± 13%

* The dose rate values for the source height were multiplied by the 0.73 factor obtained in 2016.
** Given that the ion chamber CST and H_2O values are statistically equivalent, it is appropriate to use the mean value.
# This mean dose rate for CST and H_2O using films is 6.3% less than that measured using ion chamber. Because the estimated total uncertainty in this value (~13%) is nearly 4X the ion chamber uncertainty (2.6%), it was determined that the dose rates and doses for the vessel contents should be based on the ion chamber measurements.

Source 318-420 was used in the Colburn/Bryan gas vessel irradiations in 2016, and data for this source was obtained during the July 3, 2018 Gamma Bunker calibrations as well in order to provide additional confidence in the dose rates associated with both 2016 and 2018 gas vessel irradiations. Note the dose rate values obtained for the average over the volume were 6.03, 5.88, and 5.61 kGy/hr for July 3, September 10, and January 20 respectively. September 10, 2018 and January 20, 2019 are the middle of those two irradiation runs and associated with the average dose rates for the runs.

Figures 3 and 4 show the Air-Kerma Rate values measured in the central axis of the vessels, and provide a dose distribution curve that can be compared to the radiochromic film measurement performed in 2016 (which represented points outside the central axis as well, and thus an average over more of the full resin and water volumes). Note that the *normalized* curves for the 2016 measurements and these July, 2018 measurements are very similar. For these July 3, 2018 data, the 0.73 factor obtained in 2016 for correcting from peak dose rate (6.75 cm height) to the average dose rate throughout the volume was used.

In addition to providing additional dose rate data for the source height position, the vertical film assemblies were also used to provide an estimate for the *dose distribution along the vertical axis of the*
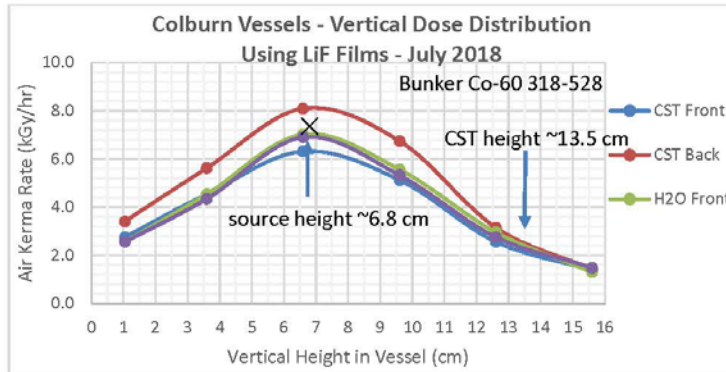
Figure 3: Plot of the measured Air-Kerma rates along the vertical axis of the gas vessels (Film results), including the A16 ion chamber (In-Air) result at source height.
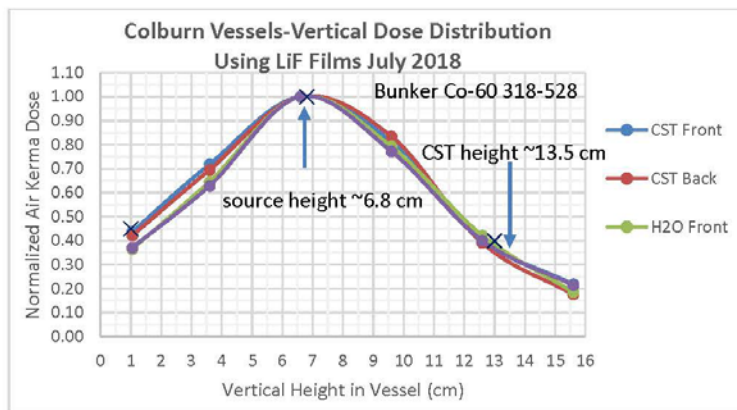
Figure 4: Same data as in Figure 3, but normalized to the dose rate at source height. Shows that the change in dose rate as the vertical height changes is very similar for all the gas vessels.

vessels. Note that the dose rate results are included for the films on front-side of PET strip and the backside of the PET strip. As can be seen from the dose rate data for source height, the difference in measured dose rate is minimal (< 2%) between the front-side and backside films for the *water-filled* vessels, while the results for the front-side and backside films for *CST-filled* vessels are significantly different (~20%). It is theorized that the lower reading of the front-side film may be due to the CST in front providing insufficient charged-particle equilibrium (CPE). If this is true, it would also provide less attenuation than the water-filled vessels. It is determined that the buildup additionally induced by the

Colburn Gamma Bunker dose characterization 24Apr2019 signed.docx   April 21, 2019

front film and the plastic strip, combined with lower-energy photons originating from the bunker chamber wall, accounts for the higher response on the backside film. The steel vessel wall should provide plenty of electrons within the vessel volume to overcome a possible lack of CPE build-up, or even provide an excess (compared to plastic), but the electron energy profile is likely different as well.

It is with high confidence that the true dose rates along the vertical axis of the CST-filled and water-filled vessels are determined to be somewhere between the front side and backside measured values, and a reasonable estimate would be the average of the two values.

Assessment of Total Dose to Gas Vessel Content for September and January Runs

The mean dose rate for the CST and H2O within the vessels, using the LiF films, is ~6.3% less than that measured using the ion chambers. Because the estimated total uncertainty in the film measured dose rates (~13%) is nearly 4X the ion chamber uncertainty (2.6%), it was determined that the dose rates and doses for the vessel contents should be based on the ion chamber measurements and not the films.

The Colburn/Bryan September 2018 gas vessel irradiation run, using cobalt-60 source 318-528, started at 10:30 AM on 8/29/2018. Given the best estimate for the July 3, 2018 measured average absorbed dose rate (relative to water) throughout the CST and water volumes provided above (6.03 kGy/hr), and correcting for radioactive decay, the resulting average dose rate is 5.88 kGy/hr. Therefore, the total integrated dose for an end date of 10:30 AM on 9/21/2018 (total 552 hours) is 3.23 MGy (323 Mrads).

The Colburn/Bryan January 2019 gas vessel irradiation run, using cobalt-60 source 318-528, started at 6:57 AM on January 9. Given the best estimate for the July 3, 2018 measured average absorbed dose rate (relative to water) throughout the CST and water volumes provided above (6.03 kGy/hr), and correcting for radioactive decay, the resulting average dose rate is 5.61 kGy/hr for the 22 day run. Therefore, the total integrated dose for an end date of 9:35 am on 1/31/2019 (total 530.6 hours) is 2.98 MGy (298 Mrad). For the same run, the total integrated dose for an end date of 7:50 am on 3/18/2019 (total 1632.8 hours) is 9.08 MGy (908 Mrad) with an average dose rate of 5.559 kGy/hr.

Uncertainties

The estimated expanded uncertainty (k=2) for the absorbed dose received by the gas vessel contents are 2.6% and 12.6% as measured by ion chamber and LiF film, respectively. These uncertainty estimates have been determined following the guidelines of Evaluation of Measurement Data – Guide to the Expression of Uncertainty in Measurement, JCGM 100:2008, and includes components evaluated by statistical means (Type-A uncertainties) and components determined on the basis of alternative methods, such as scientific judgment, calibration reports, etc. (Type-B uncertainties). To determine the expanded uncertainty, the total combined standard uncertainty is multiplied by the listed coverage factor (k) appropriate for the estimated effective degrees of freedom.

Colburn Gamma Bunker dose characterization 24Apr2019 signed.docx   April 21, 2019

Distribution List

Washington River Protection Solutions
KE Ard
BE Chamberlain
DM Ferrara
MR Landon
RD Lanning
JE Meacham
JG Reynolds
RM Russell
MG Valentine
LAWPS Documents LAWPSVENDOR@rl.gov

Savannah River National Laboratory
DT Herman
DJ McCabe

DOE – Office of River Protection
BM Crock
SC Smith

Pacific Northwest National Laboratory
SR Adami
CA Burns
SA Bryan
DM Camaioni
HA Colburn
SK Fiskum
MS Fountain
PA Gauglitz
RA Peterson
AM Rovira
PP Schonewill
Project File
Information Release (pdf)

**Pacific Northwest
National Laboratory**

902 Battelle Boulevard
P.O. Box 999
Richland, WA 99354
1-888-375-PNNL (7665)

www.pnnl.gov